Time-varying economic dominance in financial markets: A bistable dynamics approach

Xue-Zhong He, Kai Li, and Chuncheng Wang

Citation: Chaos **28**, 055903 (2018); doi: 10.1063/1.5021141
View online: https://doi.org/10.1063/1.5021141
View Table of Contents: http://aip.scitation.org/toc/cha/28/5
Published by the American Institute of Physics

Time-varying economic dominance in financial markets: A bistable dynamics approach

Xue-Zhong He,[1,a)] Kai Li,[1,2,b)] and Chuncheng Wang[3,c)]
[1]*UTS Business School, University of Technology Sydney, PO Box 123, Broadway, NSW 2007, Australia*
[2]*Institute of Financial Studies, Southwestern University of Finance and Economics, Chendu, China*
[3]*Department of Mathematics, Harbin Institute of Technology, Harbin, China*

(Received 2 January 2018; accepted 27 March 2018; published online 16 May 2018)

By developing a continuous-time heterogeneous agent financial market model of multi-assets traded by fundamental and momentum investors, we provide a potential mechanism for generating time-varying dominance between fundamental and non-fundamental in financial markets. We show that investment constraints lead to the coexistence of a locally stable fundamental steady state and a locally stable limit cycle around the fundamental, characterized by a Bautin bifurcation. This provides a mechanism for market prices to switch stochastically between the two persistent but very different market states, leading to the coexistence and time-varying dominance of seemingly controversial efficient market and price momentum over different time periods. The model also generates other financial market stylized facts, such as spillover effects in both momentum and volatility, market booms, crashes, and correlation reduction due to cross-sectional momentum trading. Empirical evidence based on the U.S. market supports the main findings. The mechanism developed in this paper can be used to characterize time-varying economic dominance in economics and finance in general. *Published by AIP Publishing*. https://doi.org/10.1063/1.5021141

In this paper, a continuous-time heterogeneous agent model (HAM) of multi-assets traded by fundamental and momentum investors is formulated. Bifurcation analysis is carried out by center manifold theorem and normal form theory, and the results indicate that this nonlinear model tends to have a locally stable steady state and a limit cycle simultaneously. Triggered by random shocks, the solutions may switch stochastically between these two attractors. Empirical evidence based on U.S. market supports the main findings. The model provides a potential mechanism in generating time-varying dominance between fundamental and non-fundamental in financial markets and also generates other financial market stylized facts. This paper is closely related to the momentum and heterogeneous agent model (HAM) literature and we conduct an analysis of global dynamics, which complements the local stability analysis well documented in the HAM literature. This provides a better understanding of the complexity and the underlying economic mechanism of market behavior.

I. INTRODUCTION

The coexistence of puzzling and even controversial financial market anomalies and hypotheses is well documented. This is perfectly reflected by different views of the 2013 Nobel Laureates Eugene Fama and Robert Shiller on efficient market hypothesis. As one of the most important paradigms in finance, the efficient market theory argues that information is incorporated into prices efficiently (Fama, 1970; 2014). In contrast, Shiller (2003; 2014) views financial markets from a broader social science perspective, including psychology and sociology, and develops a behavioral approach to explaining inefficiency of financial markets such as bubbles, crashes, and excess volatility. This stands in sharp contradiction to much of the efficient market theory. Very often, we observe a time-varying dominance among the two controversial views; financial markets are more efficient over certain time periods but less efficient in other time periods. The questions are how to characterize such time-varying dominance and what is the underlying mechanism for such wildly observed coexistence in financial markets. In this paper, we provide a general framework to answer these questions. We develop a continuous-time financial market model with heterogeneous agents who trade multi-assets based on either economic fundamentals or price momentums to characterize the coexistence of such controversial views on market efficiency and time-varying dominance of one over the other in different time periods in financial markets. From a globally nonlinear dynamics point of view, we show that investment constrains can cause the coexistence of two different and locally stable market states. It is such coexistence, together with random shocks, that underlies the time-varying dominance of different market states in financial markets.

By incorporating investment constraints, we model asset prices as nonlinear interaction of agents who trade on fundamentals and agents who trade on price momentum (either in time series or cross-section). The two trading behavior of agents are motivated by return reversal and momentum in the cross-section well documented in financial markets. The resulting asset price model tends to have bistable dynamics,

[a)]tony.he1@uts.edu.au
[b)]kai.li@uts.edu.au
[c)]Author to whom correspondence should be addressed: wangchuncheng@hit.edu.cn

characterized by a Bautin bifurcation, in which a locally stable fundamental steady state coexists with a locally stable limit cycle around the fundamental. Depending on market price levels and random shocks, market prices display two very different market states. One characterizes small deviations of market price from the fundamental price, leading market prices to be more efficient; while the other characterizes cyclical fluctuations around the fundamental price, enhancing cross-sectional price momentum and leading to less efficient markets. Triggered by random shocks, market prices then switch stochastically between the two persistent market states (due to their local stability), leading to the coexistence of seemingly controversial efficient market and price momentum over different time periods.

To explore the underlying mechanism on the coexistence, we conduct a detailed analysis of the global dynamics of the nonlinear financial market model and provide better understanding of the complexity of market behavior. The analysis complements the local stability analysis approach well used in the extant nonlinear economic model literature. By applying the normal form method and center manifold theory, we demonstrate bistable dynamics (the coexistence of a locally stable steady state and a locally stable limit cycle) through a Bautin bifurcation (generalized Hopf bifurcation). [The Bautin bifurcation is similar to the Chenciner bifurcation in discrete-time model, which is used to explain the volatility clustering observed in various financial markets, see Gaunersdorfer *et al.* (2008) and He *et al.* (2016).] We provide analytical conditions for the bistable dynamics and show that both time series and cross-sectional momentum can lead to bistable dynamics. The Bautin bifurcation is characterized numerically by conditions in which a Hopf bifurcation occurs and meanwhile, the first Lyapunov coefficient, which determines the direction and stability of the Hopf bifurcation, is zero. With the aid of the Matlab package DDE-BIFTOOL, we numerically study the global extension of the bifurcated periodic solutions, track unstable limit cycles, and provide the condition for bistable dynamics.

The current agent based financial market literature is mainly based on local stability analysis of the fundamental steady state. It focuses on the forward and stable bifurcated cycles around the fundamental steady state characterized by the negative Lyapuniv coefficient. However, when the first Lyapunov coefficient is positive, the Hopf bifurcation is backward and the bifurcated periodic solution becomes unstable. In this case, the bifurcated unstable periodic solution can be extended backward with respect to the bifurcation parameter until a threshold value and then, the extended periodic solution becomes forward (with respect to the bifurcation parameter) and stable. Therefore, the stable fundamental steady state can coexist with the stable forward extended periodic solution, in between the backward extended periodic solution which is unstable. Correspondingly, there exists an interval for the bifurcation parameter in which the two locally stable attractors coexist. This implies that, even when the fundamental steady state is locally stable, prices need not converge to the fundamental value, but may settle down to a stable limit cycle, depending on the initial price levels. The stylized approach for the global dynamics analysis employed and the underlying mechanism in this paper can be used to characterize the time-varying economic dominance in general.

The impact of cross-sectional momentum trading on the bistable dynamics is investigated through three scenarios. (i) In the first scenario, two separate risky asset prices have forward and stable bifurcations before introducing cross-sectional momentum trading among two risky assets. When agents are allowed to trade two risky assets at the same time via the cross-sectional momentum trading, the two assets are integrated into one market. We show that the newly integrated market can only generate forward and stable bifurcations. (ii) In the second scenario when the two prices have backward and unstable bifurcations before integration, the integrated market can have either backward (unstable) bifurcation or forward (stable) bifurcation. (iii) In the third scenario when one risky price has backward (unstable) bifurcation and the other has forward (stable) bifurcation, the integrated market can also have either backward (unstable) bifurcation or forward (stable) bifurcation. The analysis of the above scenarios shows that in addition to reducing the local stability of the steady states (meaning a smaller local stability parameter region or basin of the attraction), the momentum trading can enhance the local stability of the limit cycles (meaning a larger parameter region or basin of the attraction for the bifurcated period solution). This provides another channel through which momentum trading can destabilize the market. More specifically, we show that the cross-sectional momentum trading tends to destabilize the local stability of the fundamental steady state by reducing the parameter region of the local stability and enhance cyclical price oscillation around the fundamental steady state.

Intuitively, the bistable dynamics is caused by the constraints faced by both fundamental and momentum investors. On the one hand, various constraints faced by the fundamental traders, such as the wealth and short-sale constraints, limit the activity of the fundamental traders. This reduces the size of the basin of the attraction of the stable fundamental steady state. When the initial values are far away from the steady state, the prices tend to depart further away from the steady state. On the other hand, the wealth and short-sale constraints also limit the destabilizing role of the momentum investors. As a result, the prices cannot explode but settle down at a stable cycle around the fundamental steady state. Therefore, the constraints limit the strengths of both local attractors (the stable steady state and the stable limit cycle), resulting in bistable dynamics.

Our results lead to several empirical implications. First, we find that a strong integration via the cross-sectional momentum results in comovements in asset prices in opposite directions. Second, cross-sectional momentum trading can give rise to a spillover effect in momentum, which is documented empirically in Gebhardt *et al.* (2005) and Jostova *et al.* (2013), and can reduce the correlation of stock returns. More interestingly, the model suggests that cross-sectional momentum trading tends to be self-fulfilling in the sense that it destabilizes the market and generates additional price trends in cross-section. Furthermore, we provide empirical evidence based on the U.S. market to support the reduction in return correlation. We find that an increase in the

usage of cross-sectional momentum strategies significantly decreases the correlations among stocks by 35% on average after Jegadeesh and Titman published their seminal work in 1993. Also the profits of the cross-sectional momentum increase by 1.5%. The empirical findings are consistent with our analytical results.

This paper is closely related to the momentum literature. Momentum profitability is found to depend on market states (Chordia and Shivakumar, 2002; Cooper *et al*., 2004), investor sentiment (Antoniou *et al*., 2013), and market volatility (Wang and Xu, 2015). For example, Cooper *et al*. (2004) found that short-run (six months) momentum strategies are profitable in an up-market, but no in a down-market. Recently, Daniel and Moskowitz (2016) documented that the momentum strategy tends to experience severe crashes during market rebounds. Chu *et al*. (2015) showed that the dominance of fundamental and behavioral-bias-related nonfundamental strengths is time-varying. [He *et al*. (2018) show that studying both fundamental and momentum jointly is more powerful than examining each in isolation.] However, most existing theories are independent of market conditions either implying a long-lasting momentum or ruling out the existence of momentum. They are difficult to harmonize with the time-varying existence of momentum. In our model, the "inefficient" momentum and "efficient" market price can coexist. Their dominance depends on the price levels (and price shocks).

This paper is also related to heterogeneous agent models (HAM) literature. Over the last three decades, empirical evidence, unconvincing justification of the assumption of unbounded rationality, and investor psychology have led to the growing research on HAMs. [See Hommes (2006), LeBaron (2006), Chiarella *et al*. (2009), Lux (2009), He (2013), and Dieci and He (2018) for surveys of the recent development in this literature.] With different groups of investors having different expectations about future prices, HAMs have shown that asset price fluctuations can be caused by an endogenous mechanism of interaction of heterogeneous agents (Brock and Hommes, 1997; 1998; Chiarella *et al*., 2002). Given the complexity of nonlinear financial markets, most of the HAMs are computationally oriented based on local stability and bifurcation analysis, while the globally nonlinear properties are seldom analyzed (through the normal form method and the center manifold theory). He *et al*. (2009; 2016) are two exceptions. In addition to the local stability analysis, He *et al*. (2009) analytically examine the bifurcation properties, including the direction of the bifurcation, the stability of the bifurcated cycle, and the global extension of the bifurcated cycle. He *et al*. (2016) further provide the conditions of Chenciner bifurcation and show the coexistence of two local attractors. This paper conducts a global dynamics analysis, which complements the local stability analysis well documented in HAM literature. It provides better understanding of the complexity and the underlying economic mechanism of market behavior. This paper also contributes to the studies of interactions between financial markets by examining the effects of the cross-sectional momentum trading on both local and global dynamics and a large set of stylized facts in financial markets. The interaction among financial markets has also been demonstrated by a number of earlier HAMs, including Westerhoff (2004), Chiarella *et al*. (2005), Chen and Huang (2008), Marsili *et al*. (2009), Dieci and Westerhoff (2010), Schmitt and Westerhoff (2014) and Dieci *et al*. (2018). In particular, Westerhoff (2004) considers a multi-asset model with fundamentalists who concentrate only on one market and trend followers who invest in all markets; Dieci and Westerhoff (2010) explore deterministic models to study two stock markets denominated in different currencies, which are linked via the related foreign exchange market; Chen and Huang (2008) develop a computational multi-asset artificial stock market to examine the relevance of risk preferences and forecasting accuracy to the survival of investors; Marsili *et al*. (2009) introduce a generic model of a multi-asset financial market to show that correlation feedback can lead to market instability when trading volumes are high. Schmitt and Westerhoff (2014) calibrate their model to match a number of important stylized facts of financial markets, including comovements and cross-correlations; and Dieci *et al*. (2018) develop a framework with countercyclical asset price dynamics.

The bistable dynamics is related to the multiple equilibria mechanism in the sense that a nonlinear financial market can have multiple locally stable attractors. However, different from the multiple equilibria mechanism, the two attractors in our mechanism are very different. Therefore, the model is able to characterize seemingly unrelated or even opposite market phenomena, such as price momentum and efficient market.

This paper is organized as follows. We first propose a continuous-time heterogeneous agent model of two assets in Sec. II to explicitly characterize momentum trading. In Sec. III, we apply stability and bifurcation theory, together with the normal form method and center manifold theory, to examine both local and global dynamics of the model. In particular, we demonstrate the coexistence of a local stable fundamental price and a locally stable closed cycle around the fundamental price. Section IV conducts a numerical analysis of the stochastic model to explore the joint impact of the global deterministic dynamics and noises. Based on the U.S. market data, Sec. V provides empirical evidence to some implications of the model. Section VI concludes a more general model with multiple assets and all the proofs are included in the Appendixes.

II. THE MODEL

We consider a financial market of two risky assets (A and B), populated by fundamental investors, extrapolators, and noise traders. To have an intuitive and parsimonious model, we motivate the demand functions based on agents' behavior directly by following Chiarella (1992), He and Li (2012, 2015), and Di Guilmi *et al*. (2014). [The demands in the continuous-time setup are consistent with those deriving from heterogeneous expectations and utility maximization in discrete time HAM literature, see, for example, Brock and Hommes (1997; 1998).] The fundamental investor trade

based on the (log) book-to-market ratio and their excess demands is given by

$$D^i_{f,t} = \tanh\left[\beta_f(F^i_t - P^i_t)\right], \quad i = A, B, \tag{2.1}$$

where F^i_t and P^i_t are the log fundamental price and log market price, respectively, at time t, and $\beta_f > 0$ is a constant measuring the mean-reverting of the market price to the fundamental price. The S-shaped hyperbolic demand function $[\tanh(\cdot)]$ reflects various constraints faced by agents, such as the wealth constraint (the upper bound) and the short-sale constraint (the lower bound). For simplicity, we consider that the fundamental prices are governed by

$$\begin{pmatrix} dF^A_t \\ dF^B_t \end{pmatrix} = \Sigma^F dW^F_t, \quad \Sigma^F = \begin{pmatrix} \sigma^F_{A,1} & \sigma^F_{A,2} \\ \sigma^F_{B,1} & \sigma^F_{B,2} \end{pmatrix},$$
$$\begin{pmatrix} F^A_0 \\ F^B_0 \end{pmatrix} = \begin{pmatrix} \bar{F}^A \\ \bar{F}^B \end{pmatrix}, \tag{2.2}$$

where Σ^F is the variance-covariance matrix for fundamental returns and $W^F_t = (W^F_{1,t}, W^F_{2,t})'$ are two independent Brownian motions.

The literature has extensively documented that many individual and institutional investors extrapolate historical returns [see, e.g., Vissing-Jorgensen (2004), Bacchetta *et al.* (2009), Barberis (2013), Amromin and Sharpe (2014), Greenwood and Shleifer (2014), and Kuchler and Zafar (2016)], and shown that both time series momentum (or absolute momentum) and cross-sectional momentum (or relative momentum) widely used in practice can generate persistent and sizeable profits [see, e.g., Jegadeesh and Titman (1993) and Moskowitz *et al.* (2012) among many others]. Accordingly, we also consider extrapolators who trade on short-run price trends. The extrapolators estimate the price trend using a moving average of historical returns

$$\int_{t-\tau}^{t} dP^i_u = P^i_t - P^i_{t-\tau},$$

where dP^i_u is the (log) instantaneous return of asset i and τ is the look-back period of the extrapolation. There are two types of extrapolators, based on time series momentum and cross-sectional momentum, respectively. The demands of the absolute momentum investors for assets A and B are given, respectively, by

$$D^i_{a,t} = \tanh\left[\beta_a(P^i_t - P^i_{t-\tau})\right], \quad i = A, B, \tag{2.3}$$

where parameter $\beta_a > 0$ represents the extrapolation rate of the absolute momentum investors on the future price trend.

The cross-sectional momentum strategy has been extensively documented in the literature (e.g., Jegadeesh and Titman, 1993; 2001; Daniel and Moskowitz, 2016, among many others). It is typically conducted by longing the winners, the stocks have higher past returns relative to other stocks, and shorting the losers, the stocks have lower past returns relative to other stocks. Accordingly, the demands of the cross-sectional momentum investors are given by

$$\begin{aligned} D^A_{c,t} &= \tanh\{\beta_c\left[(P^A_t - P^A_{t-\tau}) - (P^B_t - P^B_{t-\tau})\right]\}, \\ D^B_{c,t} &= \tanh\{\beta_c\left[(P^B_t - P^B_{t-\tau}) - (P^A_t - P^A_{t-\tau})\right]\}, \end{aligned} \tag{2.4}$$

where $\beta_c > 0$ is a constant. Equation (2.4) implies that the cross-sectional momentum strategy is a zero-investment strategy by taking a long position in one asset and a short position in the other asset simultaneously. We consider the same time horizon τ for both assets to be consistent with the cross-sectional momentum literature.

Therefore, both fundamental investors and absolute momentum investors focus only on individual assets, while the cross-sectional momentum investors trade on two assets simultaneously. The market fractions of the three types of investors who trade on asset i are α^i_f, α^i_a, and α^i_c, respectively, satisfying $\alpha^i_f + \alpha^i_a + \alpha^i_c = 1$. Here, α^i_c denotes the market fraction rather than the number of traders. So it can be different for the two assets even though the cross-sectional momentum investors are the same group of investors across the two risky assets.

The market maker adjusts the market price according to the aggregated excess demand

$$\begin{aligned} dP^A_t = \mu^A \Big[& \alpha^A_f \tanh\left[\beta_f(F^A_t - P^A_t)\right] + \alpha^A_a \tanh\left[\beta_a(P^A_t - P^A_{t-\tau})\right] \\ & + \alpha^A_c \tanh\{\beta_c\left[(P^A_t - P^A_{t-\tau}) - (P^B_t - P^B_{t-\tau})\right]\}\Big] dt + \sigma^M_A dW^M_t, \\ dP^B_t = \mu^B \Big[& \alpha^B_f \tanh\left[\beta_f(F^B_t - P^B_t)\right] + \alpha^B_a \tanh\left[\beta_a(P^B_t - P^B_{t-\tau})\right] \\ & + \alpha^B_c \tanh\{\beta_c\left[(P^B_t - P^B_{t-\tau}) - (P^A_t - P^A_{t-\tau})\right]\}\Big] dt + \sigma^M_B dW^M_t, \end{aligned} \tag{2.5}$$

where the constant $\mu^i > 0$ represents the speed of the price adjustment by the market maker

$$\Sigma^M = \begin{pmatrix} \sigma^M_A \\ \sigma^M_B \end{pmatrix} = \begin{pmatrix} \sigma^M_{A,1} & \sigma^M_{A,2} \\ \sigma^M_{B,1} & \sigma^M_{B,2} \end{pmatrix}.$$

is the variance-covariance matrix for the market returns and $W^M_t = (W^M_{1,t}, W^M_{2,t})'$ represents two independent Brownian motions, measuring the demands of noise traders or market noises. They can be correlated with the fundamental shocks $W_{F,t}$; however, in the numerical analysis we assume they are independent for simplicity. Specifically, when Σ^M is a diagonal matrix, the conditional volatility of one asset cannot be affected by the other asset and hence, any spill-over effect in the realized volatility cannot be introduced by this term. However, the two assets are still linked via the fundamental correlation and the relative momentum investors.

The asset price model (2.5) is characterized by a nonlinear stochastic delay differential system. The resulting returns are linear functions of three factors, including a fundamental component and two momentum components, in addition to a noise term. In a consumption-based asset pricing model where sentiment investors extrapolate the expected returns using all historical returns, Barberis *et al.* (2015) show that the return process is linear in the dividend process and the extrapolators' belief. Empirically, Grinblatt and Moskowitz (2004) and Heston and Sadka (2008), among others, find that the historical average returns over a short-run horizon can

positively forecast return in the cross-section. In the following analysis, the local dynamics of the corresponding deterministic model is examined via the linearized form of (2.5). We show that, different from the fundamental factor, the two momentum factors tend to destabilize the market and may result in non-stationary return processes. Furthermore, the global dynamics analysis shows a rich and more complex return behavior, which goes beyond the scope of the linear models used in the empirical momentum literature.

III. DETERMINISTIC DYNAMICS

This section examines the price dynamics of the deterministic skeleton of (2.5). By assuming a constant fundamental price $F_t^i = \bar{F}^i$ and no market noise $\Sigma^M = 0$, system (2.5) becomes a deterministic system of delay differential equations, representing the mean processes of market returns of the two risky assets

$$\begin{aligned}\dot{P}_t^A &= \mu^A\Big[\alpha_f^A \tanh\Big[\beta_f(\bar{F}^A - P_t^A)\Big] + \alpha_a^A \tanh\big[\beta_a(P_t^A - P_{t-\tau}^A)\big] \\ &\quad + \alpha_c^A \tanh\{\beta_c\big[(P_t^A - P_{t-\tau}^A) - (P_t^B - P_{t-\tau}^B)\big]\}\Big], \\ \dot{P}_t^B &= \mu^B\Big[\alpha_f^B \tanh\Big[\beta_f(\bar{F}^B - P_t^B)\Big] + \alpha_a^B \tanh\big[\beta_a(P_t^B - P_{t-\tau}^B)\big] \\ &\quad + \alpha_c^B \tanh\{\beta_c\big[(P_t^B - P_{t-\tau}^B) - (P_t^A - P_{t-\tau}^A)\big]\}\Big].\end{aligned} \tag{3.1}$$

The linearization of (3.1) at its unique fundamental steady state $(P^A, P^B) = (\bar{F}^A, \bar{F}^B)$ is given by

$$\begin{aligned}\dot{P}_t^A &= (\gamma_a^A + \gamma_c^A - \gamma_f^A)P_t^A - (\gamma_a^A + \gamma_c^A)P_{t-\tau}^A - \gamma_c^A P_t^B + \gamma_c^A P_{t-\tau}^B, \\ \dot{P}_t^B &= (\gamma_a^B + \gamma_c^B - \gamma_f^B)P_t^B - (\gamma_a^B + \gamma_c^B)P_{t-\tau}^B - \gamma_c^B P_t^A + \gamma_c^B P_{t-\tau}^A,\end{aligned} \tag{3.2}$$

where $\gamma_f^i = \mu^i \alpha_f^i \beta_f$, $\gamma_a^i = \mu^i \alpha_a^i \beta_a$, and $\gamma_c^i = \mu^i \alpha_c^i \beta_c$, $i = A, B$ measure the activities of the three types of investors. Before studying the full model (3.1) with all three types of investors, we first examine several special cases to understand the roles of different types of traders.

A. Bistable dynamics of the single asset model

We first consider the case when there are no cross-sectional momentum investors, that is $\gamma_c^i = 0$. In this case, the price dynamics of the two assets is decoupled into two separate single asset price dynamics

$$\begin{aligned}\dot{P}_t^A &= \mu^A\Big[\alpha_f^A \tanh\Big[\beta_f(\bar{F}^A - P_t^A)\Big] + \alpha_a^A \tanh\big[\beta_a(P_t^A - P_{t-\tau}^A)\big]\Big], \\ \dot{P}_t^B &= \mu^B\Big[\alpha_f^B \tanh\Big[\beta_f(\bar{F}^B - P_t^B)\Big] + \alpha_a^B \tanh\big[\beta_a(P_t^B - P_{t-\tau}^B)\big]\Big].\end{aligned} \tag{3.3}$$

The local dynamics can be described as the following.

Proposition 3.1. *For system (3.3) with $i = A, B$,*

(1) *it has a unique fundamental steady state $P^i = \bar{F}^i$;*
(2) *the fundamental steady state P^i is locally asymptotically stable for all $\tau \geq 0$ when $\gamma_f^i \geq 2\gamma_a^i$;*
(3) *the fundamental steady state P^i is locally asymptotically stable for $\tau < \tau_0^i$ and unstable for $\tau > \tau_0^i$ when $\gamma_f^i < 2\gamma_a^i$. In addition, P^i undergoes Hopf bifurcations at $\tau = \tau_n^i$, $n = 0, 1, 2, \ldots$.*

There always exist multiple Hopf bifurcation values for a delayed differential system as we have here. These bifurcation values τ_n^i are usually governed by complex equations. However, the first bifurcation value is the most important because it determined the local stability of the steady state, while others have less effects on the local stability of the steady state and tend to affect global dynamics. As such, we focus on the first bifurcation value in the paper to study the effect of momentum trading on the local stability of fundamental steady state. Local dynamics has been well understood in the HAM literature. For example, He and Li (2012), among others, show that fundamental investors play a stabilizing role, while momentum investors play a destabilizing role in financial markets and the local stability can switch as the time horizon τ increases. Specifically, if neither the absolute momentum investors nor the relative momentum investors participate into the market, the fundamental steady state is always stable.

However, global price dynamics has been seldom studied in the literature [there are a few exceptions: e.g., the global extension of bifurcated cycles is studied in He *et al.* (2009; 2016); the piecewise linear maps are studied in Sushko *et al.* (2006) and Sushko *et al.* (2016)] and is still unclear so far. Therefore, we mainly focus on the coexistence of attractors of the global dynamics and the dynamic interaction between the two assets in this paper. Denote the first Lyapunov coefficient by $c_1(0)$, which is derived in Subsection 2 of the Appendix B. The stability of the Hopf bifurcation can be characterized.

Proposition 3.2. *For system (3.3) with $i = A, B$,*

(1) *if $c_1(0) = 0$, it undergoes a Bautin bifurcation (generalized Hopf bifurcation);*
(2) *if $\gamma_f^i < 2\gamma_a^i$ and $c_1(0) \neq 0$, then the direction and stability of the bifurcated periodic solutions (Hopf bifurcation) are completely determined by the sign of the first Lyapunov coefficient $c_1(0)$. That is, the bifurcated periodic solutions are forward stable when $c_1(0) < 0$, but backward and unstable when $c_1(0) > 0$.*

Figure 1 illustrates the impact of the absolute momentum trading, measured by β_a, on the global price dynamics, especially the stability of the bifurcated limit cycles. As β_a increases, the sign of the first Lyapunov coefficient $c_1(0)$ switches from positive to negative. Following Proposition 3.2, the direction of Hopf bifurcation changes from backward to forward; correspondingly, the unstable bifurcated cycle becomes stable. When the first Lyapunov coefficient $c_1(0) = 0$, system (3.3) has a Bautin bifurcation (generalized Hopf bifurcation). The occurrence of Bautin bifurcation implies that, with a proper set of parameters, a stable steady state can coexist with a stable limit cycle (a bistable dynamics, see Chap. 8 of Kuznetsov, 2004). Interestingly, numerical analysis suggests that the first Lyapunov coefficient $c_1(0)$ tends to keep the same sign as α_j^i changes. Intuitively, the right-hand side of (3.3) is linear in α_j^i, implying that α_j^i can affect the local stability of the steady state while it may not

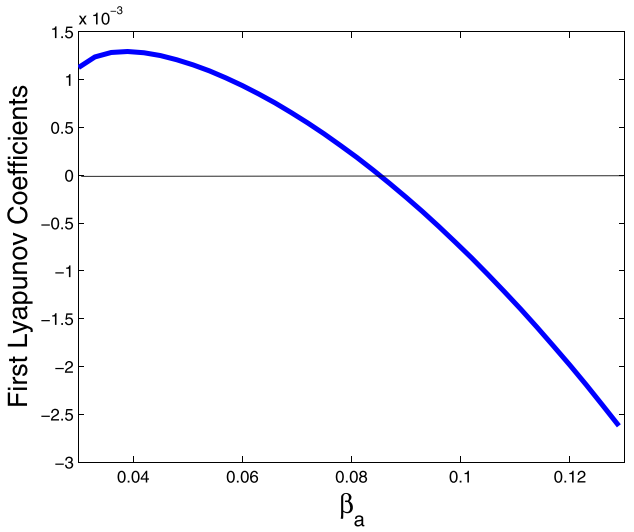

FIG. 1. The first Lyapunov coefficient as a function of β_a. Here, $\mu^i = 15$, $\alpha_f^i = 0.2$, $\alpha_a^i = 0.8$, $\alpha_c^i = 0$, $\beta_f = 0.2$, and $\tau = \tau_0^i$.

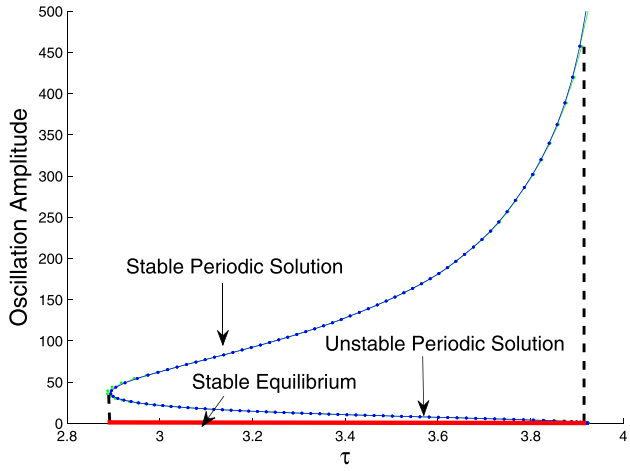

FIG. 2. The extension of the periodic solution bifurcated through a backward and unstable Hopf bifurcation. Here, $\mu = \mu^i = 15$, $\alpha_f^i = 0.2$, $\alpha_a^i = 0.8$, $\alpha_c^i = 0$, $\beta_f = 0.2$, and $\beta_a = 0.04$. The first Hopf bifurcation value $\tau_0^i \approx 3.92$ and first Lyapunov coefficient $c_1(0) = 1.3 \times 10^{-3} > 0$.

affect the stability of the bifurcation. However, (3.3) is nonlinear in β_j and hence, it can affect the global dynamics as illustrated in Fig. 1. In the following analysis, we examine two different scenarios [$c_1(0) > 0$ and $c_1(0) < 0$] separately, and show that these two scenarios have different local and global dynamics.

1. Scenario 1: $c_1(0)>0$

We set $\mu = \mu^i = 15$, $\alpha_f^i = 0.2$, $\alpha_a^i = 0.8$, $\alpha_c^i = 0$, $\beta_f = 0.2$, and $\beta_a = 0.04$. It follows from (B5) and (B11) that the first Hopf bifurcation value $\tau_0 \approx 3.92$ and first Lyapunov coefficient $c_1(0) = 1.3 \times 10^{-3} > 0$. Proposition 3.1 implies that the fundamental steady state is locally stable for $\tau < \tau_0^i$, but becoming unstable for $\tau > \tau_0^i$. Proposition 3.2 further shows that there is a backward Hopf bifurcation when $\tau = \tau_0^i$, and the corresponding bifurcated periodic solution is unstable. We numerically examine the tendency of the bifurcated periodic solution using the Matlab package DDE-BIFTOOL, which can even track the unstable limit cycles. The numerical method is described in Subsection 3 of the Appendix B. Figure 2 illustrates how the bifurcated periodic solution varies with parameter τ. Every point in the curve stands for a periodic solution, and hence, the curve is called the branch of periodic solutions [see He *et al.* (2009) for the proofs of the global extension of the Hopf bifurcation]. As τ varies, the periodic solution with small amplitude at the beginning moves to the left initially, then turns around at the critical value τ^{i*} ($\approx$2.89), and then shifts to the right. At $\tau = \tau^{i*}$, the two limit cycles collide and disappear via a saddle-node bifurcation of periodic solutions (Kuznetsov, 2004). Therefore, there are two periodic solutions coexisting for $\tau \in (\tau^{i*}, \tau_0^i)$. By further computing the corresponding nontrivial Floquet multiplier (the one with the maximal module among all multipliers) for these two periodic solutions with fixed $\tau \in (\tau^{i*}, \tau_0^i)$, we find that the periodic solution with the relatively larger amplitude is stable, while the other is unstable. Hence, when τ is within the coexistence interval, (τ^{i*}, τ_0^i), there are two local attractors, the asymptotically stable fundamental steady state and the asymptotically stable limit cycle around the fundamental steady state with larger amplitude, and in between there is an unstable cycle. As τ increases, the branch increases steeply, implying large amplitudes of the cycles. Numerical simulations (not reported here) show that an increase in β_a decreases the length of the coexistence interval.

The bistable dynamics is caused by the constrained trading activities of both fundamental and momentum investors. Intuitively, on the one hand, the fundamental investors face various constraints, such as the wealth and short-sale constraints, which limit their trading activity and reduce the size of the basin of the local attractor of the stable steady state. When the initial values are far away from the steady state, the prices tend to depart further away from the steady state. On the other hand, the wealth and short-sale constraints (or the *S*-shaped demand function) also limit the destabilizing role of the momentum investors. As a result, the prices cannot explode but settle down at a stable cycle. Therefore, the constraints limit the strengths of both local attractors (the stable steady state and the stable limit cycle), resulting in the bistable dynamics. On the one hand, we find that the limit cycles tend to be unstable and the solutions to the system can explode to infinity without the *S*-shaped demand functions of the momentum investors. On the other hand, after removing the *S*-shaped demand functions of the fundamental investors, although the limit cycles are stable, the bistable dynamics tend to disappear. In Sec. IV A, we show that, triggered by the random shocks in the stochastic model (2.5), the bistable dynamics can lead market prices to switch stochastically but persistently between the two attractors, characterizing two very different market states.

2. Scenario 2: $c_1(0)<0$

We choose $\mu = \mu^i = 15$, $\alpha_f^i = 0.2$, $\alpha_a^i = 0.8$, $\alpha_c^i = 0$, $\beta_f = 0.2$, and $\beta_a = 0.12$. In this case, the first Hopf bifurcation value is $\tau_0^i \approx 0.81$, and $c_1(0) = -2.0 \times 10^{-3} < 0$. Proposition 3.2 implies that the Hopf bifurcation is forward

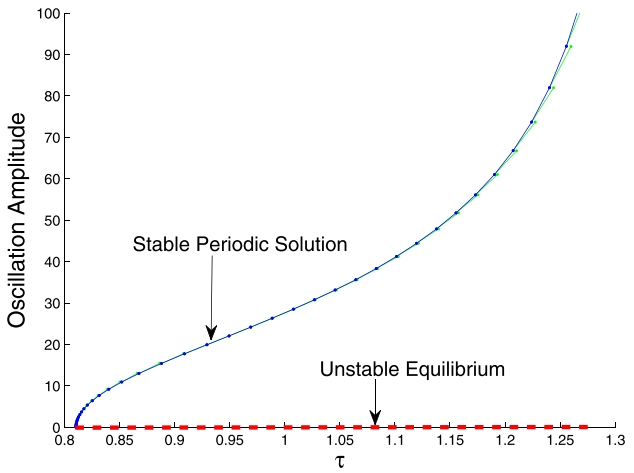

FIG. 3. The extension of periodic solution bifurcated through a forward and stable Hopf bifurcation. Here, $\mu = \mu^i = 15$, $\alpha_f^i = 0.2$, $\alpha_a^i = 0.8$, $\alpha_c^i = 0$, $\beta_f = 0.2$, and $\beta_a = 0.12$. The first Hopf bifurcation value $\tau_0^i \approx 0.81$ and first Lyapunov coefficient $c_1(0) = -2.0 \times 10^{-3} < 0$.

and stable. Figure 3 illustrates the extension of the Hopf bifurcation. The fundamental steady state is stable for $\tau < \tau_0^i$ but becomes unstable for $\tau > \tau_0^i$. The bifurcated forward limit cycles are stable and the amplitude of the cycles increases as τ increases.

We complete the discussion with the following remark. When the Hopf bifurcation is forward and stable as in Scenario 2, the oscillation amplitude of the bifurcated cycles is very small around the bifurcation value and increases with τ. However, when the Hopf bifurcation is backward and unstable as in Scenario 1, the extended bifurcated cycles have large oscillation amplitude around the bifurcation value. In other words, there is a big jump from the stable steady state to the stable cycle around the bifurcation value.

B. Bistable dynamics of the two assets model

The previous analysis shows different roles played by different types of investors. We now analyze the market stability when all three strategies are employed. The market stability of the system (3.1) can be characterized by the following proposition.

Proposition 3.3. *For system* (3.1),

(1) *it has a unique fundamental steady state* $(P^A, P^B) = (\bar{F}^A, \bar{F}^B)$;
(2) *the fundamental steady state is locally asymptotically stable for all* $\tau \geq 0$ *under condition* $\bar{\mathbf{C}}$ *defined in Subsection 6 of the Appendix B;*
(3) *the fundamental steady state is locally asymptotically stable for* $\tau \in [0, \tau_0)$ *but becomes unstable for* $\tau > \tau_0$ *under condition* $\mathbf{C}$ *in Subsection 6 of the Appendix B;*
(4) *it undergoes a Hopf bifurcation at* $\tau = \tau_0$ *under condition* $\mathbf{C}$. *In addition, if* $\frac{T}{c_1(0)} < 0$ $[\frac{T}{c_1(0)} > 0]$, *then the bifurcation is forward (backward), and the bifurcated periodic solution is stable (unstable) when* $c_1(0) < 0$ $[c_1(0) > 0]$, *where* T *and the first Lyapunov coefficient* $c_1(0)$ *are defined in Subsection 6 of the Appendix B.*

Proposition 3.3 shows that the direction and the stability of bifurcated periodic solution are determined by the sign of both the transversality condition T and the first Lyapunov coefficient $c_1(0)$. When the two individual systems are coupled together, the market integration cannot alter the fundamental steady state of each asset, while tends to destabilize the market in the sense that the integrated market is prone to be more unstable. [The effect has also been demonstrated by a number of earlier HAMs, such as Westerhoff (2004), Chiarella *et al.* (2005), Chen and Huang (2008), Marsili *et al.* (2009), Dieci and Westerhoff (2010), Schmitt and Westerhoff (2014), and Dieci *et al.* (2018)]. In the remaining analysis, we further investigate the impact of the integration on price dynamics by examining the integration strength β_c. Specifically, when there are no absolute momentum investors, that is $\alpha_a^i = 0$, Proposition 3.3 reduces to the following corollary.

Corollary 3.4. *Assume that* $\alpha_a^i = 0$ *for* $i = A, B$.

(1) *The fundamental steady state is locally asymptotically stable for all* $\tau \geq 0$ *when* $b_2 \geq 0$, *where* $b_2 = \gamma_f^A \gamma_f^B (\gamma_f^A \gamma_f^B - 2\gamma_f^A \gamma_c^B - 2\gamma_f^B \gamma_c^A)$.
(2) *The fundamental steady state is locally asymptotically stable for* $0 \leq \tau < \tau_0$ *but becomes unstable for* $\tau > \tau_0$ *when* $b_2 < 0$. *In addition, system (3.1) undergoes Hopf bifurcations at* $\tau = \tau_n$, $n = 1, 2, \ldots$, *where* τ_n *is given by (B21).*
(3) *If* $\frac{T}{c_1(0)} < 0$ $[\frac{T}{c_1(0)} > 0]$, *then the bifurcation is forward (backward), and the bifurcated periodic solution is stable (unstable) when* $c_1(0) < 0$ $[c_1(0) > 0]$, *where* T *and the first Lyapunov coefficient* $c_1(0)$ *are defined in Subsection 6 of the Appendix B.*

Figure 4 illustrates the extension of the Hopf branch bifurcated from the first bifurcation point in the (β_c, τ)-plane using DDE-BIFTOOL. The upper line is a Hopf bifurcation

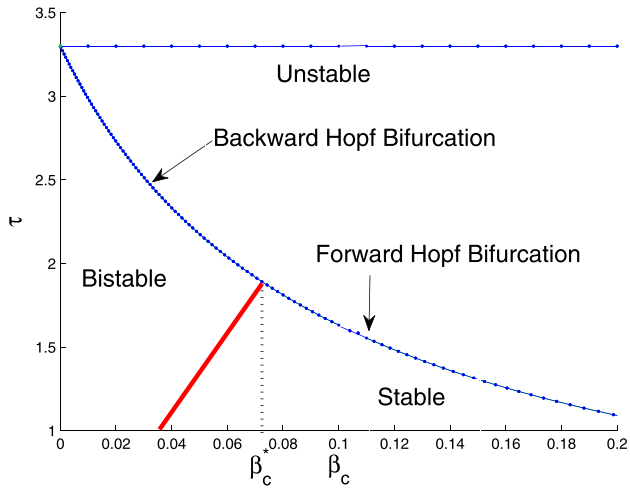

FIG. 4. The branch of Hopf bifurcation in the (τ, β_c)-plane. The upper line is a Hopf bifurcation branch, and the bifurcated periodic solution is unstable. The middle line separates the (τ, β_c)-plane into stable and unstable regions of the fundamental steady state. Through this line, backward or forward Hopf bifurcation occurs, depending on the value of β_c. For any $\beta_c < \beta_c^*$, there exists an interval for τ (as indicated by the red solid line), on which the system has bistable dynamics. Here, $\mu = 15$, $\alpha_f^A = \alpha_f^B = 0.2$, $\alpha_a^A = \alpha_a^B = 0.7$, $\alpha_c^A = \alpha_c^B = 0.1$, $\beta_a = 0.05$, and $\beta_f = 0.2$.

branch, and the bifurcated periodic solution is unstable. Its frequency (ω_2) is the same as the one for the decoupled model, and hence, the corresponding bifurcation value for τ is independent of β_c. The middle line separates the (τ, β_c)-plane into stable and unstable regions of the fundamental steady state, showing that the bifurcation value for τ decreases when β_c is increasing. Also τ tends to the bifurcation value τ_0 for the decoupled model as β_c approaches 0. Through this line, backward or forward Hopf bifurcation occurs, depending on the value of β_c. For any $\beta_c < \beta_c^*$, there exists an interval for τ (as indicated by the red solid line), on which the system has bistable dynamics characterized by the coexistence of a stable steady state and a stable cycle.

Figure 4 leads to several observations. First, the first Hopf bifurcation value in terms of τ decreases as β_c increases, see the decreasing blue line in the middle of Fig. 4. This implies that enforcing the integration strength reduces the bifurcation value. Therefore, the two assets with stable prices before integration can become unstable when they are strongly coupled. Second, the sign of the first Lyapunov coefficient $c_1(0)$ changes as the intensity of integration β_c increases and exceeds the critical value $\beta_c^* \approx 0.07$, while the quantity T does not switch sign as shown in Fig. 5. Therefore, the direction and the stability of the bifurcation change at β_c^*. Third, there is a Bautin bifurcation (generalized Hopf bifurcation) for system (3.1) at (τ_0^1, β_c^*), which theoretically implies the coexistence of two local attractors (the stable fundamental steady state and the stable limit cycle).

If both assets are unstable before coupling, then there are two series of bifurcation values introduced by the two assets, respectively, after market integration. For example, we consider $\tilde{\tau}_0^A < \tilde{\tau}_0^B$. Asset A becomes unstable when $\tau > \tilde{\tau}_0^A$. An interesting question following Proposition 3.3 would be whether asset B is still stable or becomes unstable for $\tilde{\tau}_0^A < \tau < \tilde{\tau}_0^B$ after integrated with asset A. The following corollary indicates the latter.

Corollary 3.5. *Assume* $\gamma_c^i \neq 0$. *The two prices of system (3.1) converge to their fundamental steady state prices or fluctuate cyclically simultaneously*.

We have three observations from Corollary 3.5. First, we do not have a market situation in which one asset price converges to its fundamental price (or "stable") and the other fluctuates cyclically (or "unstable") simultaneously. This is different from the observations in Chiarella *et al.* (2013) that one asset is stable and the other can be unstable in a coupled system. Intuitively, the multi-assets are coupled via the variance-covariance matrices in Chiarella *et al.* (2013), which is in the higher order terms and hence cannot affect the local stability. However, the current model couples the two assets together even in its linearization skeleton. Specifically, (3.1) can have such situation that price A is stable while price B is unstable if $\gamma_c^A = 0$, which however violates the condition in Corollary 3.5. Furthermore, when the system is unstable, the bifurcated periodic solutions of the two assets have the same period because the oscillation frequency is unique as demonstrated by Proposition 3.3.

Second, there is a spill-over effect in momentum. More specifically, consider two separate assets, one is stable and the other is unstable, that is, one has no trend and the other has (time series) momentum effect. After market integration when agents diversify their portfolios, Corollary 3.5, together with Proposition 3.4, shows that the stable asset becomes unstable and exhibits momentum. Therefore, the momentum can spill over from one asset to another. The spillover effect in momentum is also documented empirically in Gebhardt *et al.* (2005) and Jostova *et al.* (2013). This implies that time series momentum can give rise to cross-sectional momentum. In fact, Moskowitz *et al.* (2012) showed that positive autocovariance is the main driving force for time series momentum and cross-sectional momentum effects, while the contribution of serial cross-correlations and variation in mean returns is small. Furthermore, they show that time series momentum "*is able to fully explain cross-sectional momentum across all assets as well as within each asset class*," while time series momentum is not fully captured by cross-sectional momentum. Our model provides a theoretical support to these empirical findings.

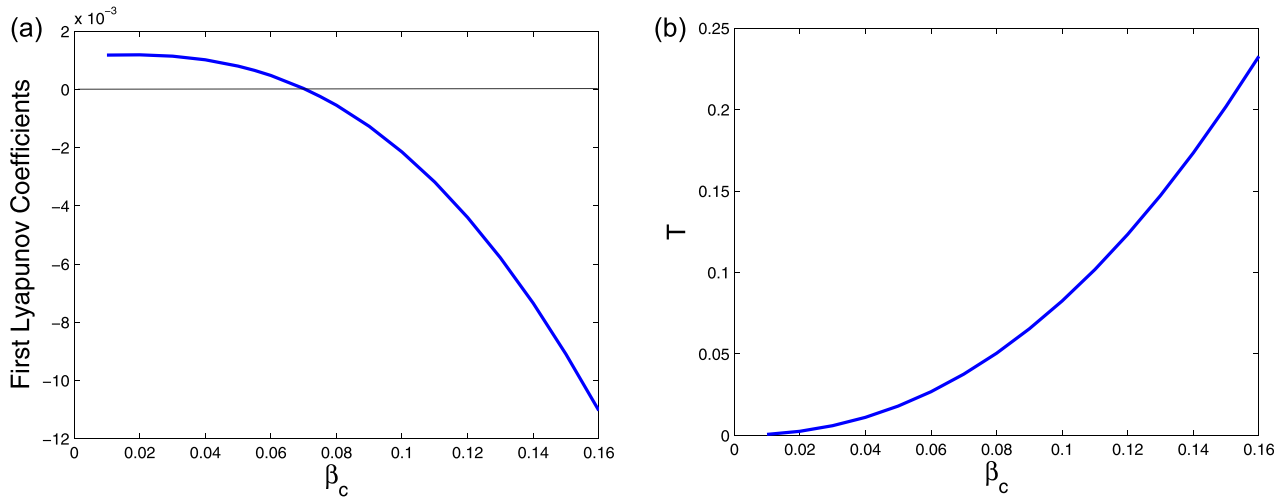

FIG. 5. (a) The first Lyapunov coefficient $c_1(0)$ and (b) the transversality condition T as functions of β_c. Here, $\mu^i = 15$, $\alpha_f^A = \alpha_f^B = 0.2$, $\alpha_a^A = \alpha_a^B = 0.7$, $\alpha_c^A = \alpha_c^B = 0.1$, $\beta_a = 0.05$, and $\beta_f = 0.2$.

Third, notice that (3.1) implies that P^A_{t+dt} (P^B_{t+dt}) is a decreasing function of P^B_t (P^A_t). An increase in one asset price tends to decrease the other's price. The countercyclical behavior of the two asset prices is caused by the cross-sectional momentum trading. In other words, cross-sectional momentum trading makes the two asset returns be negatively correlated, which in turn amplifies the cross-sectional momentum effect. Therefore, the cross-sectional momentum trading tends to be self-fulfilling. He and Li (2015) also show that the time series momentum trading is self-fulfilling. Dieci *et al.* (2018) also find the countercyclical fluctuations that is due to the market entry and exit behavior of investors. Schmitt and Westerhoff (2014) also document comovements in a multi-asset market.

In summary, we show that the cross-sectional momentum trading, which integrates the two asset dynamics, can change both local and global dynamics by making the two price dynamics resonate.

C. The impact of cross-sectional trading on the bistable dynamics

We further explore how the integration effect affects the dynamics of (3.1) by numerically studying different dynamics of the two assets before integration.

1. Scenario A: Backward + backward ⇒ backward or forward

We first examine the case in which the two prices for assets A and B have backward and unstable bifurcations before the integration. Set $\mu^i = 15$, $\alpha^A_f = 0.2$, $\alpha^B_f = 0.25$, $\beta_f = 0.2$, $\alpha^A_a = 0.7$, $\alpha^B_a = 0.65$, and $\beta_a = 0.05$. By Propositions 3.1 and 3.2, the first bifurcation values for each asset model are 3.30 (for A) and 5.21 (for B) and their first Lyapunov coefficients are 1.1×10^{-3} and 1.2×10^{-3}, respectively, implying backward and unstable bifurcations for each asset before the integration. Let $\alpha^A_c = 0.1$, $\alpha^B_c = 0.1$ and $\beta_c = 0.03$. Then, there are two frequencies $\omega_1 \approx 0.59$ and $\omega_2 \approx 0.46$ for the integrated system, and their corresponding smallest bifurcation values are $\tau^1_0 \approx 2.74$ and $\tau^2_0 \approx 4.42$, respectively. Therefore, the first Hopf bifurcation value for (3.1) is $\tau_0 = \tau^1_0$, implying that the integration effect destabilizes the fundamental steady state by reducing the first bifurcation value. Furthermore, we have $T \approx 0.02$ and $c_1(0) \approx 1.0 \times 10^{-3}$ when $\tau = \tau_0$. This indicates that the Hopf bifurcation for the integrated system (3.1) at $\tau = \tau_0$ is still backward and the bifurcated periodic solution is unstable. The bistable dynamics (one locally stable fundamental steady state and one locally stable limit cycle) is illustrated in Fig. 6 by choosing different initial values. The opposite price dynamics for the two assets are caused by the cross-sectional momentum trading, which always longs one asset while at the same time shorts the other. In other words, the cross-sectional momentum investors tend to destabilize the cross-section of asset returns.

Changing the value of parameter β_c from 0.03 to 0.09, the first bifurcation value becomes 1.86, the transversality condition $T = 0.08$, and the first Lyapunov coefficient $c_1(0) \approx -6.0 \times 10^{-4}$. This implies that the bifurcation becomes forward and the bifurcated periodic solution is stable. The bifurcation diagrams for different β_c are shown in Fig. 7. Note that the first Lyapunov coefficients are positive for both assets when they are decoupled, which may become negative after the integration. In this case, the integrated system only has one local attractor (periodic solution), even if there are two stable attractors (fundamental steady state and periodic solution) for each asset before the integration. Therefore, the integration of the two assets tends to stabilize the otherwise unstable cycles before the integration.

Intuitively, the cross-sectional momentum trading tends to destabilize the market and strengthen the stability of the limit cycles. Therefore, as the integration strength increases, the basin of the attractor of the limit cycle grows while that of the steady state declines. With a strong integration, the steady state completely losses its stability and hence the backward and unstable Hopf bifurcations for the two individual assets before the integration become forward and stable after coupling.

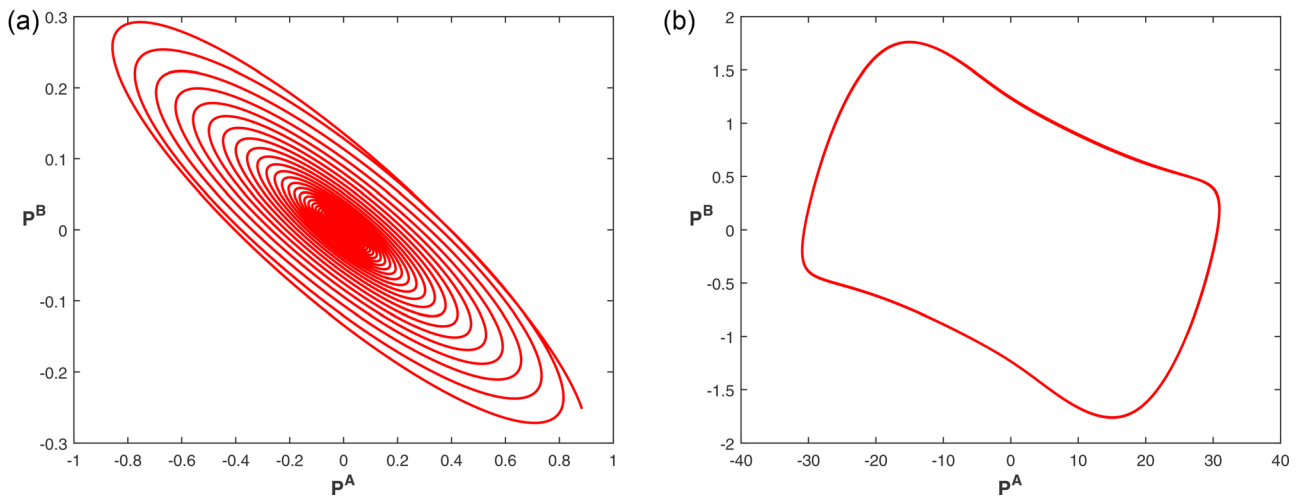

FIG. 6. The solution of (3.1) for $\tau = 2.7 < 2.74$ with different initial values: (a) $(P^A, P^B) = (2, 2)$ and (b) $(P^A, P^B) = (20, 20)$ over $[-\tau, 0]$. Here $\mu^i = 15$, $\alpha^A_f = 0.2$, $\alpha^B_f = 0.25$, $\beta_f = 0.2$, $\alpha^A_a = 0.7$, $\alpha^B_a = 0.65$, $\beta_a = 0.05$, $\alpha^A_c = 0.1$, $\alpha^B_c = 0.1$, $\beta_c = 0.03$, $\bar{F}^A = 0$ and $\bar{F}^B = 0$.

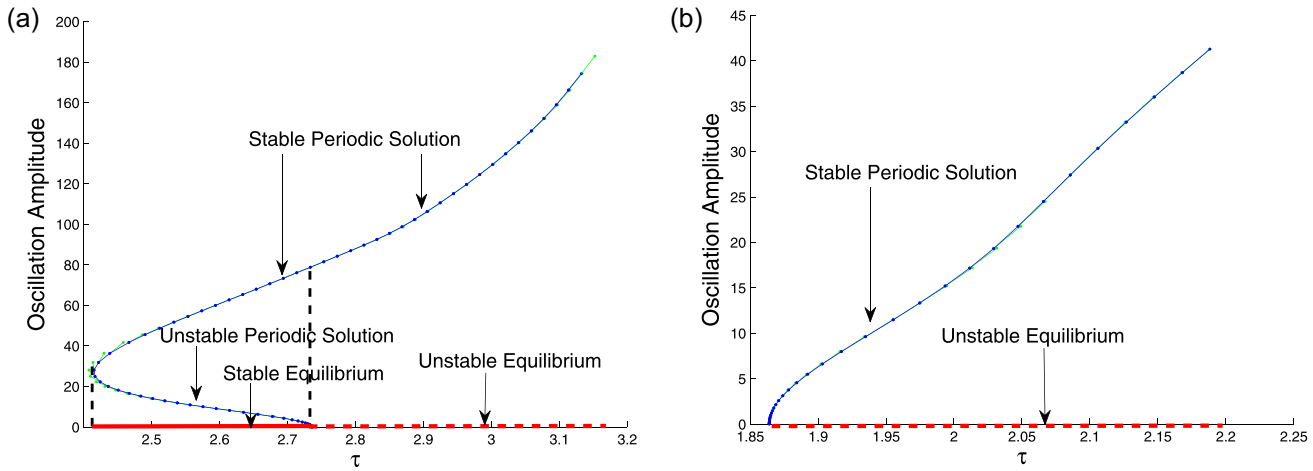

FIG. 7. Hopf bifurcation extension for asset A's price of the system (3.1) in scenario A for (a) $\beta_c = 0.03$ and (b) $\beta_c = 0.09$. Here $\mu^i = 15$, $\alpha_f^A = 0.2$, $\alpha_f^B = 0.25$, $\alpha_a^A = 0.7$, $\alpha_a^B = 0.65$, $\alpha_c^A = 0.1$, $\alpha_c^B = 0.1$, $\beta_f = 0.2$, and $\beta_a = 0.05$.

2. Scenario B: Backward + forward ⇒ backward or forward

We choose another set of parameter values, $\mu^i = 15$, $\alpha_f^A = 0.12, \alpha_f^B = 0.1, \beta_f = 0.2$, $\alpha_a^A = 0.78, \alpha_a^B = 0.3, \beta_a = 0.084$, such that each asset model undergoes different types of Hopf bifurcations when they are decoupled. In fact, the first bifurcation value and the first Lyapunov coefficient are 1.16 (3.69) and -6.4×10^{-6} (5.4×10^{-5}), respectively, for asset A (B), implying that the bifurcation is forward and stable (backward and unstable) for asset A (B). Let $\alpha_c^A = 0.1$, $\alpha_c^B = 0.6$, and $\beta_c = 0.01$. Then, there exist two frequencies $\omega_1 \approx 0.79$ and $\omega_2 \approx 0.53$, with their corresponding bifurcation values given by $\tau_0^1 \approx 1.07$ and $\tau_0^2 \approx 1.95$ for the integrated system. Moreover, $T \approx 0.07$ and $c_1(0) \approx 5.6 \times 10^{-5}$ when $\tau = \tau_0 = \tau_0^1$, which implies that the Hopf bifurcation for (3.1) at $\tau = \tau_0$ is backward and the bifurcated periodic solution is unstable. However, the first bifurcation value decreases after the integration.

Choosing $\beta_c = 0.06$, we obtain the first bifurcation value of 0.90, the transversality condition $T = 0.08$, the first Lyapunov coefficient $c_1(0) \approx -8.0 \times 10^{-4}$, and hence, the corresponding bifurcation is forward and stable. The bifurcation diagrams are similar to Fig. 7. Therefore, we show that Backward + Forward ⇒ Backward. However, the first bifurcation value becomes smaller after the integration.

3. Scenario C: Forward + forward ⇒ forward

Numerical simulations (not reported here) also show that when the two asset prices have forward and stable Hopf bifurcation before the integration, the integrated system always has a forward and stable Hopf bifurcation.

In conclusion, we have shown that the integration effect destabilizes the system in two ways. First, an increase in the integration strength parameter β_c reduces the first bifurcation value, so the fundamental steady state of the integrated system is prone to be unstable compared to the decoupled systems. Second, an increase in β_c tends to lead the cycles of the integrated system to be stable, even though the decoupled systems have unstable cycles.

IV. PRICE BEHAVIOUR OF THE STOCHASTIC MODEL

In this section, through numerical simulations, we examine the interaction between the global dynamics of the deterministic model and noise processes and explore the potential power of the model to generate various market behaviour and the stylized facts observed in financial markets.

A. Bistable dynamics and stochastic switching

Figure 8 illustrates the time series of the log market prices and log fundamental prices for assets A and B with different initial conditions. With the chosen parameters, Fig. 5 shows that the corresponding deterministic system has bistable dynamics, that is, the coexistence of a stable fundamental steady state and a stable cycle. When we choose the initial values close to the fundamental steady state, the prices converge to the stable fundamental steady state of the corresponding deterministic system. For the stochastic system, Figs. 8(a) and 8(b) show that the stochastic market prices (the red solid line) follow the fundamental prices (the blue dotted line) in general, but accompanied by small deviations from time to time. However, when we choose the initial values far away from the steady state, the prices converge to the stable limit cycle of the corresponding deterministic system and the stochastic market prices fluctuate widely around their fundamentals for the stochastic system as illustrated in Figs. 8(c) and 8(d). This illustrates a significant impact of the initial value on the price dynamics when the underlying deterministic model is bistable. Therefore, our model allows the coexistence of puzzling and even controversial financial market anomalies (efficient markets and momentum phases).

B. Spillover effect

The spillover effects in returns and volatilities have been extensively documented in the literature. It has been observed in various assets, including international equity markets (King*et al.*, 1994; Forbes and Rigobon, 2002), bond markets (Christiansen, 2007), foreign exchange markets (Hong, 2001), and commodity markets (Nazlioglu *et al.*, 2013).

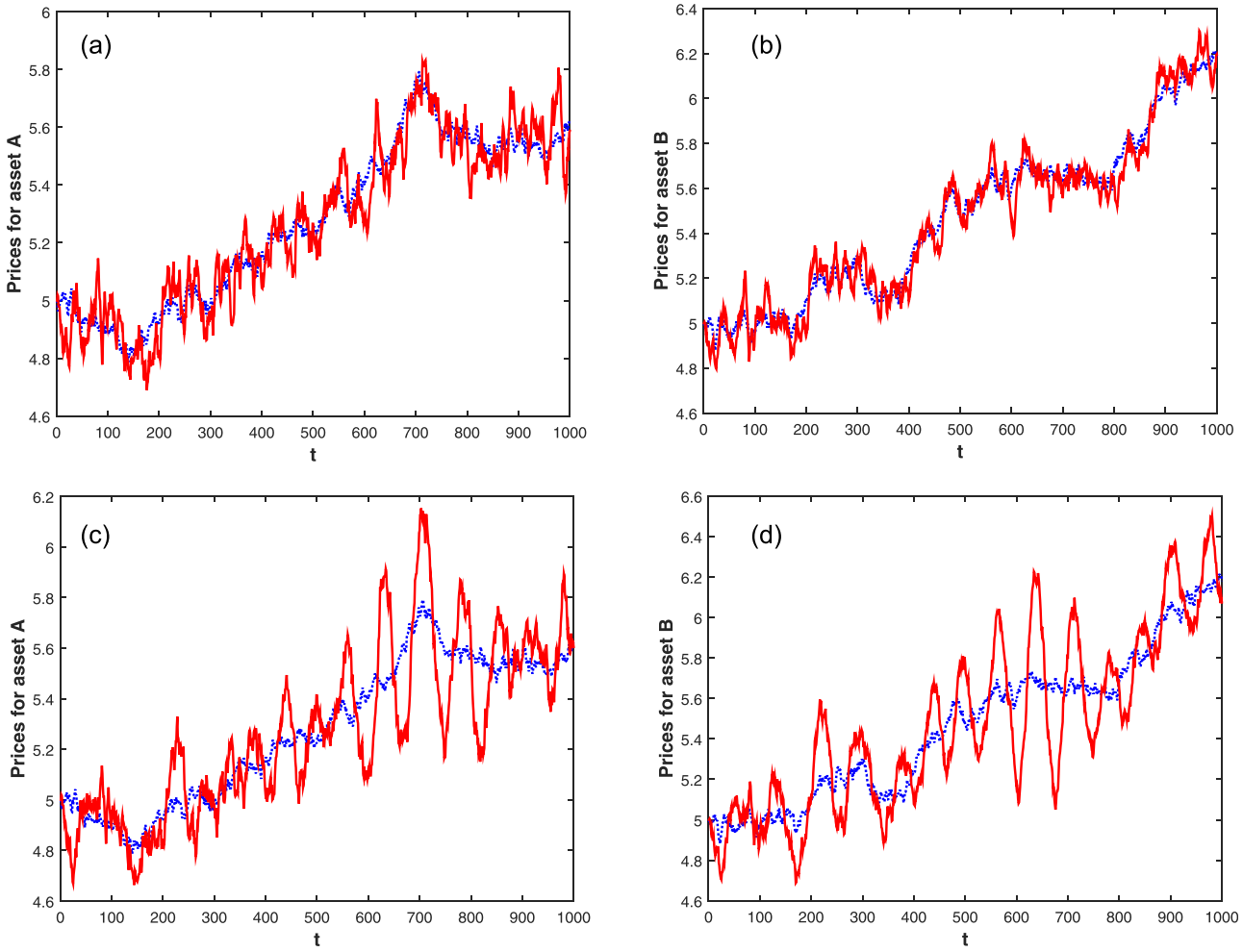

FIG. 8. The time series of log market prices and log fundamental prices for assets A and B with different initial conditions. $\mu^A = \mu^B = 15$, $\alpha_f^A = \alpha_f^B = 0.2$, $\alpha_a^A = \alpha_a^B = 0.7$, $\alpha_c^A = \alpha_c^B = 0.1$, $\beta_f = 0.2$, $\beta_a = 0.05$, $\beta_c = 0.01$, $\sigma_{A,1}^F = 0.05$, $\sigma_{A,2}^F = 0.01$, $\sigma_{B,1}^F = 0.01$, $\sigma_{B,2}^F = 0.06$, $\sigma_{A,1}^M = 0.1$, $\sigma_{A,2}^M = 0.05$, $\sigma_{B,1}^M = 0.05$, $\sigma_{B,2}^M = 0.08$, $\bar{F}^A = \bar{F}^B = 5$ and $\tau = 2$. (a) Initial value of $P_s^A = P_s^B = 2$ for $-\tau \le s \le 0$. (b) Initial value of $P_s^A = P_s^B = 2$ for $-\tau \le s \le 0$. (c) Initial value of $P_s^A = P_s^B = 20$ for $-\tau \le s \le 0$. (d) Initial value of $P_s^A = P_s^B = 20$ for $-\tau \le s \le 0$.

We numerically examine the spillover effect by exploring the joint impact of the integration intensity β_c and the two noise processes on the market price dynamics. To examine the impact of the market integration on the stochastic price dynamics, we choose the same market volatility and fundamental volatility for the two assets. Under parameters used in Fig. 9, the variance of the market noise for each asset is $0.08^2 + 0.05^2 = 8.9 \times 10^{-3}$, the covariance of the market noises for the two assets is $0.08 \times 0.05 + 0.05 \times 0.08 = 8 \times 10^{-3}$, the variance of the fundamental noise for each asset is $0.06^2 + 0.05^2 = 6.1 \times 10^{-3}$, and the covariance of the fundamental noises for the two assets is $0.06 \times 0.05 + 0.05 \times 0.06 = 6 \times 10^{-3}$. However, we consider a situation in which the fundamental steady state of the corresponding deterministic model is unstable for asset A but stable for asset B before the market integration (that is, $\beta_c = 0$). Figures 9(a) and 9(b) show that the stochastic price of asset A has greater fluctuations than asset B, and the realized annual standard deviations of market returns are 9.3% and 8.6% for assets A and B, respectively, and the correlation is 45.3%. The higher volatility for asset A is mainly driven by the greater activity of momentum investors in asset A. Figures 9(c) and 9(d) illustrate the prices after the market integration (that is, $\beta_c > 0$). They illustrate that the market integration increases the volatilities for both assets, and the realized annual standard deviations of market returns become 10.8% and 10.7% for assets A and B, respectively. Notice that the volatility for asset B increases by 24.4%, much higher than the increase for asset A, 16.1%. Therefore, cross-momentum trading leads to a spillover in volatility. However, the correlation between the two assets' returns reduces to 15.7%. In fact, Fig. 6 has shown that the cross-sectional momentum trading leads to an opposite movements of the two assets, and hence, we observe smaller correlations after market integration. Therefore, the cross-sectional momentum trading reduces return correlations, which in turn make the momentum portfolios become more diversified. Further numerical simulations (not reported here) show that the correlation increases in σ_F^{AB} and σ_M^{AB}.

We also conduct Monte Carlo simulations. Based on the set of parameters used in Fig. 9 and 1000 different random seeds, the average realized annual standard deviations of market returns are 8.9% and 8.5% for assets A and B, respectively, and the correlation is 43.5% when $\beta_c = 0$. With the cross-sectional momentum trading ($\beta_c = 0.015$), the average realized annual standard deviations of market returns

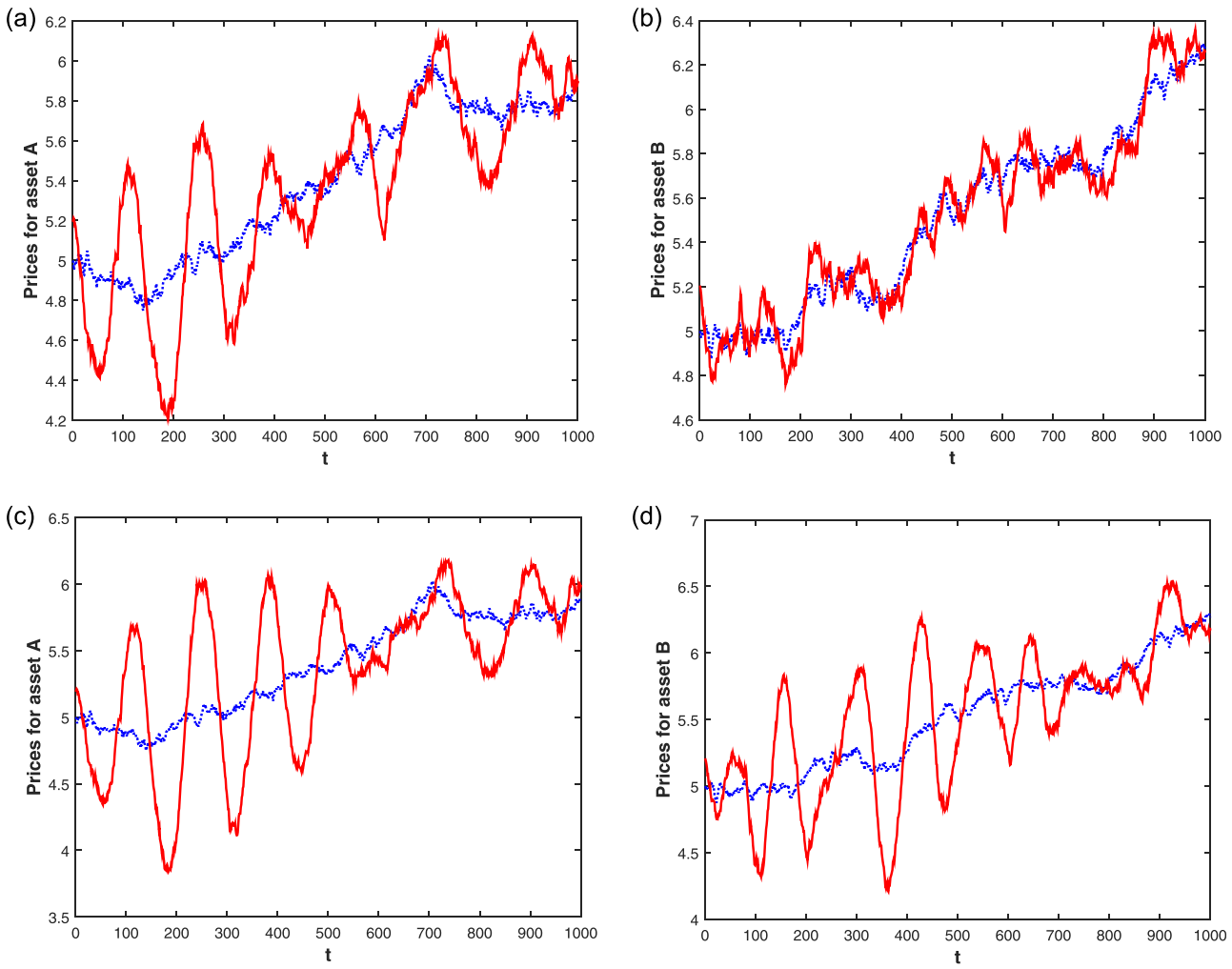

FIG. 9. The time series of log market prices and log fundamental prices for assets A and B with different initial conditions. $\mu^A = \mu^B = 15$, $\alpha_f^A = 0.2$, $\alpha_f^B = 0.7$, $\alpha_a^A = 0.7$, $\alpha_a^B = 0.2$, $\alpha_c^A = 0.1$, $\alpha_c^B = 0.1$, $\beta_f = 0.2$, $\beta_a = 0.05$, $\sigma_{A,1}^F = 0.06$, $\sigma_{A,2}^F = 0.05$, $\sigma_{B,1}^F = 0.05$, $\sigma_{B,2}^F = 0.06$, $\sigma_{A,1}^M = 0.08$, $\sigma_{A,2}^M = 0.05$, $\sigma_{B,1}^M = 0.05$, $\sigma_{B,2}^M = 0.08$, $\bar{F}^A = \bar{F}^B = 5$, and $\tau = 2.8$. (a) Prices for A when $\beta_c = 0$. (b) Prices for B when $\beta_c = 0$. (c) Prices for A when $\beta_c = 0.015$. (d) Prices for B when $\beta_c = 0.015$.

become 16.4% and 16.3% for assets A and B, respectively, and the correlation is reduced to 28.3%. The Monte Carlo results confirm that cross-sectional momentum trading reduces return correlation.

Therefore, channelled by the underlying deterministic dynamics, the stochastic price model can generate various stylized facts observed in the financial markets, including market booms and crashes, comovements, and spillover effects.

V. EMPIRICAL EVIDENCE FROM THE U.S. MARKET

Finally, we provide empirical analysis to test these model implications developed in Sec. IV. First, we examine if cross-sectional momentum trading tends to reduce the correlations among stocks. It is reasonable to assume that there would be an increase in the usage of cross-sectional momentum strategies after Jegadeesh and Titman published their seminal work in March 1993. In fact, Jegadeesh and Titman (2001) showed that the momentum strategies continued to be profitable and that past winners outperformed past losers by about the same magnitude after the publication of their 1993 paper. [Mclean and Pontiff (2016) find a decrease of 58% in the portfolio returns of 97 variables shown by academic studies to predict cross-sectional returns after they were published academically.] We examine the correlations among stock returns before and after the publication of momentum. We use the stocks listed in the S&P 100 index during 03/1986-12/2015 from CRSP. We drop the stocks with less than five years data before or after 03/1993. The correlations among each two stocks are calculated for before publication (i.e., 03/1986–02/1993) and after publication (i.e., 04/1993-12/2015). There are 76 stocks considered, implying 2850 correlations in total. We find that the distribution of the correlations is very close to a normal distribution. Panel (A) of Table I reports the average correlations before and after publication, and their difference. There is an economically and statistically significant decrease (35%) in the average correlations after the publication of momentum in 03/1993. The empirical finding is consistent with our theoretical results.

Second, our model implies that the cross-sectional momentum trading is self-fulfilling in the sense that it amplifies the price trends in cross-section. We consider the momentum portfolios constructed in Daniel and Moskowitz

TABLE I. Panel (A): the average correlations among stock returns before and after publication of momentum, and their difference. Panel (B): the average momentum profits before and after publication. *t*-statistics are reported.

	Before	After	Difference
(A) Correlation	27.1%	17.5%	−9.6%
	(111.01)	(80.87)	(−35.78)
(B) Return	20.4%	21.9%	1.5%
	(6.79)	(2.78)	

(2016). The 10-decile momentum portfolios are formed on the basis of cumulative log returns from months $t-12$ through $t-2$ using NYSE, AMEX, and NASDAQ stocks over 01/1927-03/2013. The portfolios are value weighted and rebalanced at the end of each month [see the online appendix of Daniel and Moskowitz (2016) for the details of portfolio formation]. We escape the momentum crashes periods of 07-08/1932, and 03-05/2009 documented in Daniel and Moskowitz (2016). Panel (B) of Table I shows that the annualized average returns to momentum strategies are 20.4% and 21.9%, respectively, before and after the publication of momentum, indicating an increase in 1.5% in momentum return after publication. This is consistent with the finding in Schwert (2003) that among different financial anomalies, momentum is the only persistent anomaly even after its publication. In fact, the abnormal returns even increase after its publication. Jegadeesh and Titman (2001) also showed that the relative returns to high-momentum stocks increased after their publication of momentum. We also find similar results (not reported here) based on the 10-decile momentum portfolios in Ken French's data library. (The portfolios are constructed using NYSE prior 2–12 months return decile breakpoints. See http://mba:tuck:dartmouth:edu=pages=faculty=ken:french=datalibrary:html.) Therefore, more momentum trading seems not able to arbitrage away the abnormal momentum returns and however in turn amplifies the momentum profits. This supports our model implication that the cross-sectional momentum trading destabilizes the market and leads to more significant price trends in the cross-section.

VI. CONCLUSION

In this paper, we develop a continuous-time nonlinear heterogeneous agent model of multiple assets to characterize the cross-sectional momentum trading. Both local and global dynamics are examined via stability, bifurcation theory, normal form method, and center manifold theory, respectively. The impact of the integration is examined for different cases in which the asset dynamics has various combinations before introducing cross-section momentum trading. The bistable dynamics (or the coexistence of a local stable fundamental steady state and a local stable cycle) occurs through a Bautin bifurcation (generalized Hopf bifurcation). We show that, in addition to the loss of local stability of the fundamental steady states, momentum trading destabilizes the market by strengthening the stability of limit cycles.

Channelled by the underlying deterministic dynamics, the stochastic price model can generate various stylized facts observed in financial markets, including market booms and crashes, comovements, and spillover effects. Our analysis suggests that cross-sectional momentum trading tends to be self-fulfilling in the sense that it destabilizes the market and amplifies the price trends in the cross-section. Our analysis also suggests that cross-sectional momentum trading leads to decreases in return correlations, which in turn make the cross-sectional momentum portfolios more diversified. Empirical evidence based on the U.S. market supports our main findings.

This paper studies the nonlinear effect caused by investment constraints. A model extension in which traders switch between strategies will enable us to examine the joint impact of switching and investment constraints on bistable dynamics. We leave this for future research.

ACKNOWLEDGMENTS

Financial support from the Australian Research Council (ARC) under Discovery Grants (DP130103210 and DE180100649) and the National Natural Science Foundation of China (NSFC) Grants (Nos. 11671110, 11201097, 71320107003, and 11461024) is gratefully acknowledged. The usual caveats apply.

APPENDIX A: GENERAL MODEL WITH *N* ASSETS

The two-asset model (2.5) can be extended to a general case with N risky assets

$$dP_t^i = \mu^i \left\{ \alpha_f^i \tanh(\beta_f f_t^i) + \alpha_a^i \tanh(\beta_a r_{t,t-\tau}^i) + \alpha_c^i \tanh\left[\frac{\beta_c}{N}(r_{t,t-\tau}^i - r_{t,t-\tau}^m)\right] \right\} dt + \sigma_M^A dW_{M,t}^A, \quad i = 1, 2, \ldots, N, \tag{A1}$$

where $f_t^i = F_t^i - P_t^i$ is the fundamental factor, $r_{t,t-\tau}^i = P_t^i - P_{t-\tau}^i$ is the return of asset i over the period of $[t-\tau, t]$, and $r_{t,t-\tau}^m = \sum_{i=1}^N r_t^i$ is the equally weighted market return. That is, the cross-sectional momentum investors buy the past winners and short the past losers over the period of $[t-\tau, t]$ simultaneously. Notice that the cross-sectional momentum portfolio is an arbitrage portfolio since the total investment at time t sum to zero (Lo and Mackinlay, 1990; DeMiguel *et al.*, 2014). Our analysis can be straightforwardly extended to this general case, but with a more involved results.

APPENDIX B: PROOFS

The characteristic equation at the fundamental steady state of the system (3.1) is given by

$$\left[\lambda + \gamma_f^A - (\gamma_a^A + \gamma_c^A)(1 - e^{-\lambda\tau})\right]\left[\lambda + \gamma_f^B - (\gamma_a^B + \gamma_c^B)(1 - e^{-\lambda\tau})\right] - \gamma_c^A \gamma_c^B (1 - e^{-\lambda\tau})^2 = 0. \tag{B1}$$

1. Proof of Proposition 3.1

It is easy to verify that (3.1) has a unique steady state $P^i = \bar{F}^i$. The characteristic equation reduces to

$$\lambda + \gamma_f^i - \gamma_a^i + \gamma_a^i e^{-\lambda\tau} = 0. \tag{B2}$$

When $\tau = 0$, (B2) has only one negative root $\lambda = -\gamma_f^i < 0$. Substitute $\lambda = i\omega$ ($\omega > 0$) into (B2)

$$\cos\omega\tau = 1 - \frac{\gamma_f^i}{\gamma_a^i}, \quad \sin\omega\tau = \frac{\omega}{\gamma_a^i}, \tag{B3}$$

leading to

$$\omega^2 = \gamma_f^i(2\gamma_a^i - \gamma_f^i). \tag{B4}$$

If $\gamma_f^i \geq 2\gamma_a^i$, then (B4) has no solution.

If $\gamma_f^i < 2\gamma_a^i$, then $\omega = \sqrt{\gamma_f^i(2\gamma_a^i - \gamma_f^i)}$ and

$$\tau_n^i = \frac{1}{\omega}\left[\cos^{-1}(1 - \gamma_f^i/\gamma_a^i) + 2n\pi\right], \quad n = 0, 1, 2, \ldots. \tag{B5}$$

It is easy to verify that $\frac{d(\mathrm{Re}\lambda)}{d\tau}|_{\lambda=i\omega} = \omega^2 + (\gamma_f^i - \gamma_q^i)^2 > 0$.

Therefore, the fundamental steady state P^i is locally asymptotically stable $\tau < \tau_0^i$ and unstable for $\tau > \tau_0^i$. P^i undergoes Hopf bifurcations at $\tau = \tau_n^i$, $n = 0, 1, 2, \ldots$.

2. Proof of Proposition 3.2

For the no relative momentum case, we conduct symbolic computation of the first Lyapunov coefficient, which determines the direction and stability of bifurcated periodic solutions. In this case, the prices are decoupled and the system (3.1) is given by

$$\dot{P}_t^i = \mu^i\left[\alpha_f^i \tanh\left[\beta_f(\bar{F}^i - P_t^i)\right] + \alpha_a^i \tanh\left[\beta_a(P_t^i - P_{t-\tau}^i)\right]\right], \quad i = A, B, \tag{B6}$$

which involves two analogical equations with different coefficients. In the following analysis, we drop the superscript i to get a scalar equation, which can represent any equation in (B6)

$$\dot{P}_t = \mu^i\left[\alpha_f \tanh\left[\beta_f(\bar{F} - P_t)\right] + \alpha_a \tanh[\beta_a(P_t - P_{t-\tau})]\right]. \tag{B7}$$

After a change of variable, $\hat{P}_t = P_t - \bar{F}$, and drop the "ˆ" for ease of notation, we get

$$\dot{P}_t = -\mu^i\alpha_f \tanh(\beta_f P_t) + \mu\alpha_a \tanh[\beta_a(P_t - P_{t-\tau})]. \tag{B8}$$

Taylor expanding the righthand side of (B8) at 0, and then writing its linear and nonlinear parts in functional form yield

$$\begin{aligned} L(\phi) &:= (\gamma_a - \gamma_f)\phi(0) - \gamma_a\phi(-\tau), \\ F(\phi) &:= \frac{1}{3}(\gamma_f\beta_f^2 - \gamma_a\beta_a^2)\phi^3(0) + \frac{1}{3}\gamma_a\beta_a^2\phi^3(-\tau) \\ &\quad + \gamma_a\beta_a^2\phi^2(0)\phi(-\tau) - \gamma_a\beta_a^2\phi(0)\phi^2(-\tau). \end{aligned}$$

There are mainly two methods for the first Lyapunov coefficient calculation in the literature: one is to compute the expression of center manifold (Guckenheimer and Holmes, 1983; Hassard *et al.*, 1981), and the other is to get the normal form directly via a sequence of transformation of variables without computing center manifold (Faria and Magalhaes, 1995). We use the first method by following the algorithm developed in Guckenheimer and Holmes (1983) below, which requires computing the following quantities in the first place:

(1) the matrix-valued function $\Phi(\theta)$, satisfying $A\Phi(\theta) = \Phi(\theta)B$, where A is the infinitesimal generator of the linearized equation of (B8), defined by

$$A\phi = \begin{cases} \phi'(\theta), & \theta \in [-\tau, 0), \\ (\gamma_a - \gamma_f)\phi(0) - \gamma_a\phi(-\tau), & \theta = 0, \end{cases}$$

and

$$B = \begin{pmatrix} 0, & \omega \\ -\omega, & 0 \end{pmatrix};$$

(2) the matrix-valued function $\Psi(\xi)$, satisfying $A^*\Psi(\xi) = B\Psi(\xi)$ and $(\Psi, \Phi) = I$, where A^* is the formal adjoint operator of A, defined by

$$A^*\psi = \begin{cases} -\psi'(\xi), & \xi \in (0, \tau], \\ (\gamma_a - \gamma_f)\psi(0) - \gamma_a\psi(\tau), & \xi = 0, \end{cases}$$

and $(\cdot, \cdot)$ is the bilinear form defined by

$$(\psi, \phi) = \psi(0)\phi(0) - \int_{-\tau}^{0}\int_{\xi=0}^{\theta}\psi(\xi - \theta)d\eta(\theta)\phi(\xi)d\xi;$$

(3) and the Taylor expansion, up to the second order, of the expression for center manifold: $h = h_{11}(\theta)u_1^2 + h_{12}(\theta)u_1u_2 + h_{22}(\theta)u_2^2 + O(\|\mathbf{u}\|^3) := h_2 + O(\|\mathbf{u}\|^3)$, where $\mathbf{u} = (u_1, u_2)^T$ are functions of time t, standing for the coordinates of the solution to (B8) on the center manifold.

Based on these quantities, one can derive the following ordinary differential equation for $\mathbf{u}$, up to the third order, on the center manifold

$$\dot{\mathbf{u}} = B\mathbf{u} + \Psi(0)F(\Phi\mathbf{u} + h_2 + O(\|\mathbf{u}\|^3)), \tag{B9}$$

whose general form is given by

$$\begin{aligned} \dot{u}_1 &= \omega u_2 + f_{11}^1u_1^2 + f_{12}^1u_1u_2 + f_{22}^1u_2^2 + f_{111}^1u_1^3 + f_{112}^1u_1^2u_2 \\ &\quad + f_{122}^1u_1u_2^2 + f_{222}^1u_2^3 + O(4), \\ \dot{u}_2 &= -\omega u_1 + f_{11}^2u_1^2 + f_{12}^2u_1u_2 + f_{22}^2u_2^2 + f_{111}^2u_1^3 + f_{112}^2u_1^2u_2 \\ &\quad + f_{122}^2u_1u_2^2 + f_{222}^2u_2^3 + O(4). \end{aligned}$$

The coefficients in the above equation depend on Φ, Ψ, h, and the nonlinear term F of the original equation. According to the formula by Guckenheimer and Holmes (1983), the first Lyapunov coefficient is given by

$$c_1(0) = \frac{1}{8}(3f^1_{111} + f^1_{122} + f^2_{112} + 3f^2_{222}) - \frac{1}{8\omega}\left[f^1_{12}(f^1_{11} + f^1_{22}) - f^2_{12}(f^2_{11} + f^2_{22}) - 2f^1_{11}f^2_{11} + 2f^1_{22}f^2_{22}\right]. \tag{B10}$$

Remark B.1.

(1) The matrix Ψ satisfying both $A^*\Psi = B\Psi$ and $(\Psi_1, \Phi) = I$ is usually obtained by two steps: solving $A^*\Psi = B\Psi$ to get an intermediate matrix Ψ_1, and then multiplying it by a proper matrix K to make sure that $(\Psi, \Phi) = I$, that is, $\Psi = K\Psi_1$. Therefore, $K = (\Psi_1, \Phi)^{-1}$.

(2) The second order term in h satisfies the following system:

$$\frac{\partial h_2}{\partial \theta} + O(\|\mathbf{u}\|^3) = \frac{\partial h_2}{\partial u}Bu + \Phi(\theta)\Psi(0)F_2(\Phi(\theta)u) + O(\|\mathbf{u}\|^3),$$
$$L(h_2) + F_2(\Phi(\theta)u) + O(\|\mathbf{u}\|^3) = \frac{\partial h_2}{\partial u}\bigg|_{\theta=0} Bu + \Phi(\theta)\Psi(0)F_2(\Phi(\theta)u) + O(\|\mathbf{u}\|^3).$$

which yields a series of differential equations for $h_{ij}(\theta)$, $i,j = 1,2$, with proper boundary conditions, and hence, the approximate expression for h will be obtained by solving these equations.

Along with a similar Maple program, as in Campbell (2009), one can get

$$\Phi(\theta) = [\cos(\omega\theta), \sin(\omega\theta)],$$
$$\Psi(\xi) = \begin{bmatrix} \dfrac{-2\omega([\omega\tau\cos\omega\tau - \sin\omega\tau]\cos\omega\xi + \omega\tau\sin\omega\tau\sin\omega\xi)}{\gamma_a\omega^2\tau^2 + \gamma_a\cos^2\omega\tau - 2\omega^2\tau\cos\omega\tau - \gamma_a + 2\omega\sin\omega\tau} \\ \dfrac{-2\omega([\omega\tau\cos\omega\tau - \sin\omega\tau]\sin\omega\xi - \omega\tau\sin\omega\tau\cos\omega\xi)}{\gamma_a\omega^2\tau^2 + \gamma_a\cos^2\omega\tau - 2\omega^2\tau\cos\omega\tau - \gamma_a + 2\omega\sin\omega\tau} \end{bmatrix} := \begin{bmatrix} \psi_1(\xi) \\ \psi_2(\xi) \end{bmatrix},$$

and

$$h_2 = 0.$$

The second order term h_2 being zero is due to the fact that the second order derivatives of $\tanh x$ at $x = 0$ are 0. Substituting these variables into (B9), also accomplished by Maple, we get

$$f^1_{111} = \frac{1}{3}\gamma_a\beta_a^2\psi_1(0)[-1 + 3\cos\omega\tau - 3\cos^2\omega\tau + \cos^3\omega\tau] + \frac{1}{3}\gamma_f\beta_f^2\psi_1(0),$$
$$f^1_{122} = \psi_1(0)\gamma_a\beta_a^2\sin^2\omega\tau(\cos\omega\tau - 1),$$
$$f^2_{112} = -\psi_2(0)\gamma_a\beta_a^2\sin\omega\tau(\cos\omega\tau - 1)^2,$$
$$f^2_{222} = -\frac{1}{3}\gamma_a\beta_a^2\psi_2(0)\sin^3\omega\tau,$$

and all the coefficients of the second order term in (B9) are zero. It then follows form (B10) that the first Lyapunov coefficient is finally given by

$$c_1(0) = \frac{1}{4}\gamma_a\beta_a^2\psi_1(0)(2\cos\omega\tau - \cos^2\omega\tau - 1) + \frac{1}{8}\gamma_f\beta_f^2\psi_1(0) + \frac{1}{4}\gamma_a\beta_a^2\psi_2(0)\sin\omega\tau(\cos\omega\tau - 1). \tag{B11}$$

3. Numerical method of the periodic solution branch

To examine these two limit cycles numerically around the Bautin bifurcation point, the scheme is to find a proper set of parameter values under which backward Hopf bifurcation happens, and then to check how the bifurcated periodic solution varies as one of these parameters (e.g., τ) changes. The choice of parameters for backward Hopf bifurcation is based on Propositions 3.1 and 3.2, while tracking the bifurcated periodic solution can be done with the aid of a Matlab package, DDE-BIFTOOL, which allows us to analyse the stability of steady state solutions and periodic solutions, to continue steady state fold and Hopf bifurcations, and to switch, from the latter, to an emanating branch of periodic solutions (Engelborghs *et al.*, 2001). Notice that the method can even numerically simulate the unstable limit cycles.

4. Proof of Proposition 3.4

The characteristic equation at the steady state $(P^A, P^B) = (\bar{F}^A, \bar{F}^B)$ is given by

$$\left[\lambda + \gamma_f^A - \gamma_c^A(1 - e^{-\lambda\tau})\right]\left[\lambda + \gamma_f^B - \gamma_c^B(1 - e^{-\lambda\tau})\right] - \gamma_c^A\gamma_c^B(1 - e^{-\lambda\tau})^2 = 0. \tag{B12}$$

When $\tau = 0$, (B12) has two negative roots $\lambda_1 = -\gamma_f^A$ and $\lambda_2 = -\gamma_f^B$. If $\tau > 0$, then (B26) reduces to

$$\sin\omega\tau = \frac{-\omega N(K_1 - \omega^2) + K_2\omega L}{K_2^2\omega^2 + (K_1 - \omega^2)^2},$$
$$\cos\omega\tau = \frac{-L(K_1 - \omega^2) - K_2\omega^2 N}{K_2^2\omega^2 + (K_1 - \omega^2)^2},$$

where

$$L=\gamma_f^A\gamma_c^B+\gamma_f^B\gamma_c^A,\quad N=\gamma_c^A+\gamma_c^B,\quad K_1=\gamma_f^A\gamma_f^B-L,$$
$$K_2=\gamma_f^A+\gamma_f^B-N,$$

and thus ω satisfies

$$F(\bar{\omega})=\bar{\omega}^4+P_3\bar{\omega}^3+P_2\bar{\omega}^2+P_1\bar{\omega}+P_0=0, \tag{B13}$$

with $\bar{\omega}=\omega^2$ and

$$P_3=2(K_2^2-2K_1)-N^2,$$
$$P_2=2K_1^2+(K_2^2-2K_1)^2-L^2-(K_2^2-2K_1)N^2,$$
$$P_1=2K_1^2(K_2^2-2K_1)-K_1^2N^2-(K_2^2-2K_1)L^2,$$
$$P_0=K_1^2(K_1^2-L^2).$$

We rewrite (B13) as

$$F_1(\bar{\omega})F_2(\bar{\omega})=0, \tag{B14}$$

where

$$F_1=(\bar{\omega}-\gamma_f^A\gamma_f^B+\gamma_f^A\gamma_c^B+\gamma_c^A\gamma_f^B)^2+\bar{\omega}(\gamma_f^A-\gamma_c^A+\gamma_f^B-\gamma_c^B)^2,$$
$$F_2=\bar{\omega}^2+\bar{\omega}(\gamma_f^{A2}-2\gamma_f^A\gamma_c^A+\gamma_f^{B2}-2\gamma_f^B\gamma_c^B)$$
$$+\gamma_f^A\gamma_f^B(\gamma_f^A\gamma_f^B-2\gamma_f^A\gamma_c^B-2\gamma_f^B\gamma_c^A). \tag{B15}$$

Notice $F_1\geq 0$ and we only need to examine the positive roots of $F_2(\bar{\omega})=0$. We rewrite $F_2(\bar{\omega})$ as $F_2(\bar{\omega})=\bar{\omega}^2+a_2\bar{\omega}+b_2$, where

$$a_2=\gamma_f^{A2}-2\gamma_f^A\gamma_c^A+\gamma_f^{B2}-2\gamma_f^B\gamma_c^B=K_2^2-2K_1-N^2,$$
$$b_2=\gamma_f^A\gamma_f^B(\gamma_f^A\gamma_f^B-2\gamma_f^A\gamma_c^B-2\gamma_f^B\gamma_c^A)=K_1^2-L^2.$$

It is easy to verify that there is only one frequency

$$\omega_+=\left[\frac{-a_2+\sqrt{a_2^2-4b_2}}{2}\right]^{1/2}, \tag{B16}$$

if and only if

$$(a_2,b_2)\in\{a_2^2=4b_2,\,a_2<0\}\bigcup\{b_2<0\}\bigcup\{a_2<0,\,b_2=0\}, \tag{B17}$$

there are two frequencies

$$\omega_\pm=\left[\frac{-a_2\pm\sqrt{a_2^2-4b_2}}{2}\right]^{1/2}, \tag{B18}$$

if and only if

$$(a_2,b_2)\in\{a_2^2>4b_2>0,\,a_2<0\}, \tag{B19}$$

and (B15) has no positive root if and only if

$$(a_2,b_2)\in\{a_2^2<4b_2\}\bigcup\{a_2=2\sqrt{b_2}\}\bigcup\{a_2>0,\,b_2=0\}$$
$$\times\bigcup\{a_2^2>4b_2>0,\,a_2\geq 0\}. \tag{B20}$$

When $b_2\geq 0$, we get $\gamma_f^A(\gamma_f^B-2\gamma_c^B)\geq 2\gamma_f^B\gamma_c^A$ and $\gamma_f^B(\gamma_f^A-2\gamma_c^A)\geq 2\gamma_f^A\gamma_c^B$. Hence,

$$a_2=\gamma_f^A(\gamma_f^A-2\gamma_c^A)+\gamma_f^B(\gamma_f^B-2\gamma_c^B)\geq\frac{2\gamma_f^{A2}\gamma_c^B}{\gamma_f^B}+\frac{2\gamma_f^{B2}\gamma_c^A}{\gamma_f^A}>0,$$

which implies that the sets $\{(a_2,b_2):a_2<0,\,b_2=0\}$ and $\{(a_2,b_2):a_2^2>4b_2>0,\,a_2<0\}$ are empty. It also follows from (B28) that the transversality condition is determined by the sign of $F'(\omega_+^2)$, which is equal to the sign of the quantity $F_2'(\omega_+^2)$ since $F_1>0$. If $(a_2,b_2)\in\{a_2^2=4b_2,\,a_2<0\}$, then $F_2'(\omega_+^2)=2\omega_+^2+a_2=0$. Therefore, Hopf bifurcation will never happen for $(a_2,b_2)\in\{a_2^2=4b_2,\,a_2<0\}$, and hence, the sufficient condition for the occurrence of Hopf bifurcation corresponding to one frequency is $b_2<0$, under which $F_2'(\omega_+^2)=2\omega_+^2+a_2>0$.

Note that $\sin\omega\tau>0$ for all positive ω, since $K_2L-K_1N=\gamma_f^{A2}\gamma_c^B+\gamma_f^{B2}\gamma_c^A>0$. Therefore, the bifurcation values are given by

$$\tau_n=\frac{1}{\omega_+}\left[\cos^{-1}\left(\frac{-L(K_1-\omega^2)-K_2\omega^2N}{K_2^2\omega^2+(K_1-\omega^2)^2}\right)+2n\pi\right],$$
$$n=0,1,\ldots. \tag{B21}$$

The proof of the properties of Hopf bifurcation can be found in Subsection 6 of the Appendix B for the proof for the full model.

5. Proof of Proposition 3.5

It is sufficient to show that it cannot happen that one asset's price converges to its fundamental while the other's fluctuates cyclically simultaneously. Without the loss of generality, suppose P_t^A converges to its fundamental price and P_t^B fluctuates cyclically at the same time. Because P_t^B is a cycle in this case, there exist a positive number $x>0$ and a sequence of time t_k, $k=1,2,\ldots$, such that $t_k\to\infty$ as $k\to\infty$, and $|P_{t_k}^B-P_{t_k-\tau}^B|\geq x$. (We assume that τ is not equal to the multiples of the period of the cycle. Otherwise, $P_{t_k}^B-P_{t_k-\tau}^B\equiv 0$). The first equation of (3.1) is equivalent to

$$P_{t+dt}^A-\bar{F}^A=P_t^A-\bar{F}^A+\mu^A\left[\alpha_f^A\tanh\left[\beta_f(\bar{F}^A-P_t^A)\right]\right.$$
$$+\alpha_a^A\tanh\left[\beta_a(P_t^A-P_{t-\tau}^A)\right]+\alpha_c^A\tanh\left\{\beta_c\left[(P_t^A-P_{t-\tau}^A)\right.\right.$$
$$\left.\left.\left.-(P_t^B-P_{t-\tau}^B)\right]\right\}\right]. \tag{B22}$$

As $t\to\infty$, $\bar{F}^A-P_t^A\to 0$ and $P_t^A-P_{t-\tau}^A\to 0$ due to the convergence of P_t^A. So (B22) implies that, for sufficiently large k

$$|P_{t_k+dt}^A-\bar{F}^A|\approx\mu^A\alpha_c^A\tanh\{\beta_c|P_{t_k}^B-P_{t_k-\tau}^B|\}$$
$$\geq\mu^A\alpha_c^A\tanh\{\beta_c x\}>0, \tag{B23}$$

which contradicts the assumption of the convergence of P_t^A.

This completes the proof.

6. Proof of Proposition 3.3

When $\tau=0$, there are two roots, $\lambda_1=-\gamma_a^A$ and $\lambda_1=-\gamma_a^B$, for (B1), and hence, the equilibrium is locally stable. If $\pm i\omega$, $\omega>0$ are a pair of purely imaginary roots of (B1), then we have

$$\begin{aligned}&(K_1-\omega^2)+(L-2M)\cos\omega\tau+\omega N\sin\omega\tau+M\cos 2\omega\tau=0,\\&K_2\omega-(L-2M)\sin\omega\tau+\omega N\cos\omega\tau-M\sin 2\omega\tau=0.\end{aligned}\tag{B24}$$

which is equivalent to

$$\begin{aligned}&(K_1-\omega^2-M)\sin\omega\tau+K_2\omega\cos\omega\tau+\omega N=0,\\&(K_1-\omega^2+M)\cos\omega\tau-K_2\omega\sin\omega\tau+(L-2M)=0.\end{aligned}\tag{B25}$$

Here,

$$\begin{aligned}L&=\gamma_f^A(\gamma_a^B+\gamma_c^B)+\gamma_f^B(\gamma_a^A+\gamma_c^A),\\M&=\gamma_a^A\gamma_a^B+\gamma_a^A\gamma_c^B+\gamma_c^A\gamma_a^B,\\N&=\gamma_a^A+\gamma_c^A+\gamma_a^B+\gamma_c^B,\\K_1&=\gamma_f^A\gamma_f^B-L+M,\\K_2&=\gamma_f^A+\gamma_f^B-N.\end{aligned}$$

Therefore,

$$\begin{aligned}\sin\omega\tau&=\frac{-\omega N(K_1-\omega^2+M)+K_2\omega(L-2M)}{K_2^2\omega^2+(K_1-\omega^2)^2-M^2},\\\cos\omega\tau&=\frac{-(L-2M)(K_1-\omega^2-M)-K_2\omega^2N}{K_2^2\omega^2+(K_1-\omega^2)^2-M^2}.\end{aligned}\tag{B26}$$

This implies that ω must satisfy the following equation:

$$\begin{aligned}&\left[-N(K_1-\omega^2+M)+K_2(L-2M)\right]^2\omega^2\\&\quad+\left[(L-2M)(K_1-\omega^2-M)+K_2\omega^2N\right]^2\\&\quad=\left[K_2^2\omega^2+(K_1-\omega^2)^2-M^2\right]^2,\end{aligned}$$

which can be simplified to

$$F(\bar\omega):=\bar\omega^4+P_3\bar\omega^3+P_2\bar\omega^2+P_1\bar\omega+P_0=0,\tag{B27}$$

with $\bar\omega=\omega^2$, and

$$\begin{aligned}P_3&=2(K_2^2-2K_1)-N^2,\\P_2&=2(K_1^2-M^2)+(K_2^2-2K_1)^2-(L-2M)^2\\&\quad-(K_2^2-2K_1)N^2+2MN^2,\\P_1&=2(K_1^2-M^2)(K_2^2-2K_1)-N^2(K_1+M)^2\\&\quad-(L-2M)^2(K_2^2-2K_1)-2M(L-2M)^2\\&\quad+4K_2MN(L-2M),\\P_0&=(K_1-M)^2(K_1+M)^2-(K_1-M)^2(L-2M)^2,\end{aligned}$$

The fundamental theorem of algebra suggests that (B27) has four roots. The expressions of the four roots, first proposed by Lodovico Ferrari, are extremely complicated. A detailed discussion on the conditions for different cases and the corresponding solutions would be tediously long. Therefore, instead of providing complete conditions of all possible combinations of parameters, including those economically meaningless parameter sets, we just give some simple discussions on the properties of the roots of (B27) to provide a better understanding of the roots, and then we numerically examine the roots for certain sets of parameters we are interested in. We refer readers to the study by Abramowitz and Stegun (1972) for the details of the formulas of the four roots. First, Vieta's Formulas show that (B27) has an even (odd) number of positive roots if $P_0>0$ (<0). Therefore, if $P_0<0$, (B27) has at least one positive root and hence system (3.1) will undergo Hopf bifurcations. Especially, if $P_0=0$, then the number of positive roots is determined by P_2. Second, we can rewrite (B27) as

$$(\bar\omega^2+a_1\bar\omega+b_1)(\bar\omega^2+a_2\bar\omega+b_2)=0,$$

where a_i and b_i satisfy

$$\begin{aligned}&P_0=b_1b_2,\quad P_1=a_1b_2+a_2b_1,\quad P_2=a_1a_2+b_1+b_2,\\&P_3=a_1+a_2.\end{aligned}$$

Therefore, we can instead examine the roots of the more familiar quadratic equations and the number of positive roots of (B27) is completely determined by a_i and b_i, $i=1,2$. More specifically, first, (B27) has four positive roots if and only if $\mathbf{C}_1\bigcap\mathbf{C}_2$, where $\mathbf{C}_i:=\{a_i<0\}\bigcap\{a_i^2\geq 4b_i>0\}$, $i=1,2$. The condition $\mathbf{C}_1\bigcap\mathbf{C}_2$ is equivalent to $\{P_0>0, P_1<0, P_2>0, P_3<0\}\bigcap\{a_i^2\geq 4b_i, i=1,2\}$. Second, (B27) has two positive roots if and only if $(\mathbf{C}_1\bigcap\overline{\mathbf{C}_2})\bigcup(\mathbf{C}_2\bigcap\overline{\mathbf{C}_1})$, where the overline is a complementary set operator. Third, (B27) has no positive root if and only if $\overline{\mathbf{C}_1}\bigcap\overline{\mathbf{C}_2}$. Similarly, we can determine the conditions that (B27) has one or three roots. To save space, we omit them. We denote $\bar{\mathbf{C}}:=\overline{\mathbf{C}_1}\bigcap\overline{\mathbf{C}_2}$ as the condition that (B27) has no positive root, so the parameter set $\mathbf{C}$ corresponds to the condition that (B27) has at least one positive root.

Now, we consider the properties of Hopf bifurcation of system (3.1). Assume that (B27) has positive roots, (that is, under condition $\mathbf{C}$), denoted by $\bar\omega_i$, i takes the integers from 1 to 4 depending on how many roots (B27) may have. For each $\bar\omega_i$, one can get a sequence of bifurcation values for time delay, τ_n^i, $n=0,1,\ldots$, from (B26). Denote the smallest τ_0^i for all possible i by τ_0 and the corresponding frequency by ω_0. To verify the transversality condition, set

$$\begin{aligned}G(\lambda,\tau)=&\left[\lambda+\gamma_f^A-(\gamma_a^A+\gamma_c^A)(1-e^{-\lambda\tau})\right]\\&\times\left[\lambda+\gamma_f^B-(\gamma_a^B+\gamma_c^B)(1-e^{-\lambda\tau})\right]-\gamma_c^A\gamma_c^B(1-e^{-\lambda\tau})^2.\end{aligned}$$

Using (B25), we get

$$\begin{aligned}\left.\frac{\partial G}{\partial\lambda}\right|_{\lambda=i\omega_0,\tau=\tau_0}=&\left[K_2+N\cos\omega_0\tau_0+\tau_0(K_1-\omega_0^2-M\cos 2\omega_0\tau_0)\right]\\&+i[2\omega_0-N\sin\omega_0\tau_0+\tau_0(K_2\omega_0+M\sin 2\omega_0\tau_0)],\end{aligned}$$

and

$$\left.\frac{\partial G}{\partial \tau}\right|_{\lambda=i\omega_0,\tau=\tau_0} = -\omega_0(K_2\omega_0 + M\sin 2\omega_0\tau_0) + i\omega_0(K_1 - \omega_0^2 - M\cos 2\omega_0\tau_0),$$

Therefore, $\mathrm{SignRe}\left(\frac{d\tau}{d\lambda}\right) = -\mathrm{SignRe}\left(\frac{\partial G}{\partial \lambda}/\frac{\partial G}{\partial \tau}\right)$, which equals the sign of the following quantity

$$\begin{aligned}
&\omega_0\left[K_2 + N\cos\omega_0\tau_0 + \tau_0(K_1 - \omega_0^2 - M\cos 2\omega_0\tau_0)\right](K_2\omega_0 + M\sin 2\omega_0\tau_0)\\
&\quad -\omega_0[2\omega_0 - N\sin\omega_0\tau_0 + \tau(K_2\omega_0 + M\sin 2\omega_0\tau_0)](K_1 - \omega_0^2 - M\cos 2\omega_0\tau_0)\\
&= \omega_0(K_2 + N\cos\omega_0\tau_0)(K_2\omega_0 + M\sin 2\omega_0\tau_0) - \omega_0(2\omega_0 - N\sin\omega_0\tau_0)(K_1 - \omega_0^2 - M\cos 2\omega_0\tau_0)\\
&= \omega_0^2(K_2^2 - 2K_1 + 2\omega_0^2) + \omega_0 K_2 M\sin 2\omega_0\tau_0 + 2\omega_0^2 M\cos 2\omega_0\tau_0 + K_2\omega_0^2 N\cos\omega_0\tau_0 + \omega_0 N(K_1 - \omega_0^2 + M)\sin\omega_0\tau_0\\
&= 2\omega_0^2(K_2^2 - 2K_1 + 2\omega_0^2) + 2\omega_0^2[K_2 N - (L - 2M)]\cos\omega_0\tau_0 + \omega_0\left[N(K_1 - \omega_0^2 + M) - K_2(L - 2M) - 2\omega_0^2 N\right]\sin\omega_0\tau_0\\
&= \frac{\omega_0^2(4\omega_0^6 + 3P_3\omega_0^4 + 2P_2\omega_0^2 + P_1)}{K_2^2\omega_0^2 + (K_1 - \omega_0^2)^2 - M^2} = \frac{\omega_0^2 F'(\omega_0^2)}{K_2^2\omega_0^2 + (K_1 - \omega_0^2)^2 - M^2} := T.
\end{aligned} \tag{B28}$$

The computation of $c_1(0)$ in Proposition 3.3 can be done by Maple, following the same procedure as in Subsection 2 of the Appendix B for the single asset model. However, the expression of $c_1(0)$ is much more complicated than the one for no relative momentum model, and hence it is omitted.

Remark B.2. Although we do not provide the distribution of the roots to (B27), we claim that (B27) can have positive roots for certain sets of parameters. For example, assume that $\gamma_f^A = \gamma_f^B := \gamma_f$, $\gamma_a^A = \gamma_a^B := \gamma_a$, and $\gamma_c^A = \gamma_c^B := \gamma_c$. It then follows that:

$$P_0 = \gamma_f^4(\gamma_f - 2\gamma_a - 2\gamma_c)^2\left[(\gamma_f - 2\gamma_a)^2 - 4\gamma_c(\gamma_f - 2\gamma_a)\right] > 0,$$

when $\gamma_f - 2\gamma_a < 0$. Set $\bar{\omega}_1 = \gamma_f(2\gamma_a - \gamma_f)$. We get $F(\bar{\omega}_1) = 0$ and $F'(\bar{\omega}_1) = -32\gamma_f^2\gamma_a\gamma_c^3 < 0$. Since $\lim_{\bar{\omega}\to+\infty} F(\bar{\omega}) = +\infty$, $F(\bar{\omega}) = 0$ has at least another positive solution, denoted by $\bar{\omega}_2$, which is greater than $\bar{\omega}_1$. Assume further that the two other roots of (B27) are non-positive. Then, $\bar{\omega}_1$ and $\bar{\omega}_2$ will determine two sequences of bifurcation values for τ, denoted by τ_n^1 and τ_n^2, respectively, $n = 0, 1, \ldots$, according to (B26). Recall that the decoupled system ($\gamma_c = 0$) will oscillate in one side neighborhood of τ_0^i, $i = A$ or B, if $\gamma_f - 2\gamma_a < 0$. If $\tau_0^1 < \tau_0^2$, then $\tau_0^1 (= \tau_0^i)$ is the first Hopf bifurcation value, and hence the coupled system will oscillate in the same frequency as decoupled system. While $\tau_0^1 > \tau_0^2$, the first Hopf bifurcation value becomes τ_0^2, which implies that the oscillation frequency for the coupled system is $\sqrt{\bar{\omega}_2}$. In this case, we conclude that two asset prices, oscillating in the same way (same frequency and amplitude) when decoupled, will oscillate with higher frequency after integration.

Abramowitz, M. and Stegun, I., "Solutions of quartic equations," in *Handbook of Mathematical Functions with Formulas, Graphs, and Mathematical Tables* (Dover, New York, 1972), pp. 17–18.

Amromin, G. and Sharpe, S., "From the horse's mouth: Economic conditions and investor expectations of risk and return," Manage. Sci. **60**, 845–866 (2014).

Antoniou, C., Doukas, J., and Subrahmanyam, A., "Cognitive dissonance, sentiment, and momentum," J. Financ. Quant. Anal. **48**, 245–275 (2013).

Bacchetta, P., Mertens, E., and van Wincoop, E., "Predictability in financial markets: What do survey expectations tell us?," J. Int. Money Finance **28**, 406–426 (2009).

Barberis, N., "Psychology and the financial crisis of 2007–2008," in *Financial Innovation: Too Much or Too Little?*, edited by M. Haliassos (MIT Press, Cambridge, 2013).

Barberis, N., Greenwood, R., Jin, L., and Shleifer, A., "X-CAPM: An extrapolative capital asset pricing model," J. Financ. Econ. **115**, 1–24 (2015).

Brock, W. and Hommes, C., "A rational route to randomness," Econometrica **65**, 1059–1095 (1997).

Brock, W. and Hommes, C., "Heterogeneous beliefs and routes to chaos in a simple asset pricing model," J. Econ. Dyn. Control **22**, 1235–1274 (1998).

Campbell, S., "Calculating centre manifolds for delay differential equations using maple," in *Delay Differential Equations: Recent Advances and New Directions*, edited by B. Balachandran, T. Kalmár-Nagy, and D. E. Gilsinn (Springer-Verlag, New York, 2009), pp. 221–244.

Chen, S.-H. and Huang, Y., "Risk preference, forecasting accuracy and survival dynamics: Simulations based on a multi-asset agent-based artifical stock market," J. Econ. Behav. Org. **67**, 702–717 (2008).

Chiarella, C., "The dynamics of speculative behaviour," Ann. Oper. Res. **37**, 101–123 (1992).

Chiarella, C., Dieci, R., and Gardini, L., "Speculative behaviour and complex asset price dynamics," J. Econ. Behav. Org. **49**, 173–197 (2002).

Chiarella, C., Dieci, R., and Gardini, L., "The dynamic interaction of speculation and diversification," Appl. Math. Finance **12**(1), 17–52 (2005).

Chiarella, C., Dieci, R., and He, X., "Heterogeneity, market mechanisms and asset price dynamics," in *Handbook of Financial Markets: Dynamics and Evolution*, edited by T. Hens and K. R. Schenk-Hoppe (Elsevier, 2009), pp. 277–344.

Chiarella, C., Dieci, R., He, X., and Li, K., "An evolutionary CAPM under heterogeneous beliefs," Ann. Finance **9**, 185–215 (2013).

Chordia, T. and Shivakumar, L., "Momentum, business cycle, and time-varying expected returns," J. Finance **57**, 985–1019 (2002).

Christiansen, C., "Volatility-spillover effects in European bond markets," Eur. Financ. Manage. **13**, 923–948 (2007).

Chu, L., He, X., Li, K., and Tu, J., "Market sentiment and paradigm shifts in equity premium forecasting," QFRC Working Paper No. 356 (UTS, 2015).

Cooper, M., Gutierrez, R., and Hameed, A., "Market states and momentum," J. Finance **59**, 1345–1365 (2004).

Daniel, K. and Moskowitz, T., "Momentum crashes," J. Financ. Econ. **122**, 221–247 (2016).

DeMiguel, V., Nogales, F., and Uppal, R., "Stock return serial dependence and out-of-sample portfolio performance," Rev. Financ. Stud. **27**, 1031–1073 (2014).

Di Guilmi, C., He, X., and Li, K., "Herding, trend chasing, and market volatility," J. Econ. Dyn. Control **48**, 349–373 (2014).
Dieci, R. and He, X., "Heterogeneous agent models in finance," in *Handbook of Computational Economics*, edited by C. Hommes and B. LeBaron (Elsevier, 2018), Vol. 4.
Dieci, R., Schmitt, N., and Westerhoff, F., "Interactions between stock, bond and housing markets," BERG Working Paper No. 133 (University of Bamberg, 2018).
Dieci, R. and Westerhoff, F., "Heterogeneous speculators, endogenous fluctuations and interacting markets: A model of stock prices and exchange rates," J. Econ. Dyn. Control **34**, 743–764 (2010).
Engelborghs, K., Luzyanina, T., and Samaey, G., "DDE-BIFTOOL v. 2.00: A Matlab package for bifurcation analysis of delay differential equations," Technical Report No. TW-330 (Department of Computer Science, K.U.Leuven, Leuven, Belgium, 2001).
Fama, E., "Efficient capital markets: A review of theory and empirical work," J. Finance **25**, 383–423 (1970).
Fama, E., "Two pillars of asset pricing," Am. Econ. Rev. **104**, 1467–1485 (2014).
Faria, T. and Magalhaes, L., "Normal forms for retarded functional differential equations with parameters and applications to Hopf bifurcation," J. Differ. Equations **122**, 181–200 (1995).
Forbes, K. and Rigobon, R., "No contagion, only interdependence: Measuring stock market comovements," J. Finance **57**, 2223–2261 (2002).
Gaunersdorfer, A., Hommes, C., and Wagener, F., "Bifurcation routes to volatility clustering under evolutionary learning," J. Econ. Behav. Org. **67**, 27–47 (2008).
Gebhardt, W., Hvidkjaer, S., and Swaminathan, B., "Stock and bond market interaction: Does momentum spill over?," J. Financ. Econ. **75**, 651–690 (2005).
Greenwood, R. and Shleifer, A., "Expectations of returns and expected returns," Rev. Financ. Stud. **27**, 714–746 (2014).
Grinblatt, M. and Moskowitz, T., "Predicting stock price movements from past returns: The role of consistency and tax-loss selling," J. Financ. Econ. **71**, 541–579 (2004).
Guckenheimer, J. and Holmes, P., *Nonlinear Oscillations, Dynamical Systems, and Bifurcations of Vector Fields*, Vol. 42 of Applied Mathematical Sciences (Springer, 1983).
Hassard, B., Kazarinoff, N., and Wan, Y., *Theory and Applications of Hopf Bifurcation* (Cambridge University Press, Cambridge, 1981).
He, X., "Recent developments in asset pricing with heterogeneoue beliefs and adaptive behaviour of financial markets," in *Global Analysis of Dynamic Models in Economics and Finance: Essays in Honour of Laura Gardini*, edited by G. I. Bischi, C. Chiarella, and I. Sushko (Springer, 2013), pp. 1–32.
He, X. and Li, K., "Heterogeneous beliefs and adaptive behaviour in a continuous-time asset price model," J. Econ. Dyn. Control **36**, 973–987 (2012).
He, X. and Li, K., "Profitability of time series momentum," J. Banking Finance **53**, 140–157 (2015).
He, X., Li, K., and Li, Y., "Asset allocation with time series momentum and reversal," J. Econ. Dyn. Control (2018).
He, X., Li, K., and Wang, C., "Volatility clustering: A nonlinear theoretical approach," J. Econ. Behav. Org. **130**, 274–297 (2016).
He, X., Li, K., Wei, J., and Zheng, M., "Market stability switches in a continuous-time financial market with heterogeneous beliefs," Econ. Modell. **26**, 1432–1442 (2009).
Heston, S. and Sadka, R., "Seasonality in the cross-section of stock returns," J. Financ. Econ. **87**, 418–445 (2008).
Hommes, C., "Heterogeneous agent models in economics and finance," in *Handbook of Computational Economics*, edited by L. Tesfatsion and K. L. Judd (North-Holland, 2006), Vol. 2, pp. 1109–1186; "Agent-based computational economics," in *Handbook of Computational Economics*, edited by L. Tesfatsion and K. L. Judd (North-Holland, 2006).
Hong, Y., "A test for volatility spillover with application to exchange rates," J. Econometrics **103**, 183–224 (2001).
Jegadeesh, N. and Titman, S., "Returns to buying winners and selling losers: Implications for stock market efficiency," J. Finance **48**, 65–91 (1993).
Jegadeesh, N. and Titman, S., "Profitability of momentum strategies: An evaluation of alternative explanations," J. Finance **56**, 699–720 (2001).
Jostova, G., Nikolova, S., Philipov, A., and Stahel, C., "Momentum in corporate bond returns," Rev. Financ. Stud. **26**, 1649–1693 (2013).
King, M., Sentana, E., and Wadhwani, S., "Volatility and links between national stock markets," Econometrica **62**, 901–933 (1994).
Kuchler, T. and Zafar, B., *Personal Experiences and Expectations about Aggregate Outcomes, Working Paper* (New York University/Federal Reserve Bank, New York, 2016).
Kuznetsov, Y., *Elements of Applied Bifurcation Theory* (SV, New York, 2004).
LeBaron, B., "Agent-based computational finance," in *Handbook of Computational Economics*, edited by L. Tesfatsion and K. L. Judd (North-Holland, 2006), Vol. 2, pp. 1187–1233; "Agent-based computational economics," in *Handbook of Computational Economics*, edited by L. Tesfatsion and K. L. Judd (North-Holland, 2006).
Lo, A. and Mackinlay, A., "When are contrarian profits due to stock market overreaction?," Rev. Financ. Stud. **3**, 175–205 (1990).
Lux, T., "Stochastic behavioural asset pricing and stylized facts," in *Handbook of Financial Markets: Dynamics and Evolution*, edited by T. Hens and K. R. Schenk-Hoppé (Elsevier, 2009), pp. 161–215.
Marsili, M., Raffaelli, G., and Ponsot, B., "Dynamic instability in generic model of multi-assets markets," J. Econ. Dyn. Control **33**, 1170–1181 (2009).
Mclean, R. and Pontiff, J., "Does academic research destroy stock return predictability?," J. Finance **71**, 5–32 (2016). (
Moskowitz, T., Ooi, Y., and Pedersen, L., "Time series momentum," J. Financ. Econ. **104**, 228–250 (2012).
Nazlioglu, S., Erdem, C., and Soytas, U., "Volatility spillover between oil and agricultural commodity markets," Energy Econ. **36**, 658–665 (2013).
Schmitt, N. and Westerhoff, F., "Speculative behavior and the dynamics of interacting stock markets," J. Econ. Dyn. Control **45**, 262–288 (2014).
Schwert, G., "Anomalies and market efficiency," in *Handbook of the Economics of Finance*, edited by G. M. Constantinides, M. Harris, and R. M. Stulz (North-Holland, Amsterdam, 2003).
Shiller, R., "From efficient markets theory to behavioral finance," J. Econ. Perspect. **17**, 83–104 (2003).
Shiller, R., "Speculative asset prices," Am. Econ. Rev. **104**, 1486–1517 (2014).
Sushko, I., Agliari, A., and Gardini, L., "Bifurcation structure of parameter plane for a family of unimodal piecewise smooth maps: Border-collision bifurcation curves," Chaos, Solitons Fractals **29**, 756–770 (2006).
Sushko, I., Gardini, L., and Matsuyama, K., "Robust chaos in a credit cycle model defined by a one-dimensional piecewise smooth map," Chaos, Solitons Fractals **91**, 299–309 (2016).
Vissing-Jorgensen, A., "Perspectives on behavioral finance: Does irrationality disappear with wealth? Evidence from expectations and actions," NBER Macroecon. Annu. **18**, 139–194 (2003).
Wang, K. and Xu, J., "Market volatility and momentum," J. Empirical Finance **30**, 79–91 (2015).
Westerhoff, F., "Multiasset market dynamics," Macroecon. Dyn. **8**, 591–616 (2004).